“SAPSENSE”- DEVELOPMENT OF A FIELD BASED BIOSENSOR TOWARDS WHEAT PATHOGEN DETECTION

by

Akshay Vasudevan

APPROVED BY SUPERVISORY COMMITTEE:

Shalini Prasad, Chair

Jun Wang

Vinay J. Nagaraj

To

Mandeep V Hebbar.

Shine on, you crazy diamond!

“SAPSENSE”- DEVELOPMENT OF A FIELD BASED BIOSENSOR TOWARDS WHEAT PATHOGEN DETECTION

by

AKSHAY VASUDEVAN, B.E

THESIS

Presented to the Faculty of

The University of Texas at Dallas

in Partial Fulfillment

of the Requirements

for the Degree of

MASTER OF SCIENCE IN

BIOMEDICAL ENGINEERING

THE UNIVERSITY OF TEXAS AT DALLAS

December 2017

ACKNOWLEDGEMENTS

First and foremost, I thank my advisor, Dr. Shalini Prasad, for giving me the opportunity to work at the Biomedical Microdevices and Nanotechnology Laboratory at The University of Texas at Dallas. I thank her for her support during my time as a master's student, for being my teacher, advisor and a person to look up to.

I thank Dr. Jun Wang, for his enthusiasm and encouragement for the work that was conducted during the course of this thesis. I thank Dr. Vinay Nagaraj for being patient with me, especially in rough times and encouraging me throughout the course of this project. A big thank you to my committee members.

A special thank you to Dr. Anjan Panneer Selvam, my mentor, for teaching and guiding me when I first started working in the laboratory. I thank Dr. Rajeshwari Taruvai Kalyana Kumar, for her help and support throughout my time working at BMNL.

A special thank you to Dr. Vikramshankar Kamakoti, Badrinath Jagannath and David Kinnamon for their help, advice and support. I also thank Ashlesha Bhide, Ambalika Tanak, Hunter Stevenson and all my colleagues that are a part of BMNL, for their help and support over the past year.

The biggest thank you to my parents and my brother, for their unwavering support and all the sacrifices they have had to make for my sake. Last, but certainly not the least, I thank my roommates and friends who have shared this wonderful journey with me for the last couple of years.

September 2017

“SAPSENSE”- DEVELOPMENT OF A FIELD BASED BIOSENSOR TOWARDS WHEAT PATHOGEN DETECTION

Akshay Vasudevan, MS
The University of Texas at Dallas, 2017

Supervising Professor: Shalini Prasad, PhD

Wheat is cultivated in almost all the states in the United States of America, and it is the third most cultivated crop in terms of acreage, producing a yield of 60 million tons per year. In 2016, world production of wheat was 749 million tons, making it the second most-produced cereal after maize. The most common viruses that affect wheat in the United States are Wheat Spindle Streak Mosaic Virus (WSSMV), Soil-borne Wheat Mosaic Virus (SBWMV/SBV) and the Yellow Dwarf Virus (YDF)/ High Plains Virus (HPV). Viral infections in wheat often go un-noticed due to several reasons, and cause a loss in yield and consequently a loss in revenue which is estimated at an annual average of $35 million per year, in the United States. Traditional techniques to detect these pathogens are ELISA, dot blots and PCR, all of which are time consuming and/or require benchtop laboratory equipment, and are not suitable for rapid screening.

This work aims to design and demonstrate proof of feasibility in designing a biosensor system for screening wheat viruses, through the development of a point of use system which uses the principles of electrochemical impedance spectroscopy to detect the presence of the infection

causing virus. The novelty in the proposed work is to be able to detect the virus in a standard buffer, plant sap, removing the need for any kind of filtering and processing, and thereby having the ability to detect the virus in real-time.

The biosensor works on the principles of affinity based bio-sensing with an immunoassay built on the surface of a gold electrode. Virus detection is achieved by characterizing impedance changes on the sensor surface associated with the binding of the virus to its affinity antibody probe, which is then measured by electrochemical impedance spectroscopy (EIS).

TABLE OF CONTENTS

LIST OF FIGURES

LIST OF TABLES

CHAPTER 1

INTRODUCTION

1.1 Project Aims and Goals

The overall objective of this work is to describe the detailed process in the development of a field based biosensor for the real-time detection of plant pathogen in plant sap. A two-electrode system on a Printed Circuit Board (PCB) substrate is designed and manufactured specifically for this operation. The sensing system is designed to detect the metabolite by using electrochemical studies, specifically Electrochemical Impedance Spectroscopy (EIS). Multiple Self Assembled Monolayers (SAM) are built on the surface of the sensor. The sensing will be accomplished with the detection of three viruses, namely Soil Borne Wheat Mosaic Virus (SBWMV), High Plains Virus (HPV), and Wheat Spindle Streak Mosaic Virus (WSSMV). These viruses are detected by the binding kinetics between the virus and its corresponding antibody. The pathogens chosen are the most prominent viruses that affect wheat in the United States. To achieve this overall objective, two specific aims were developed which serve as a guideline for the process of designing the entire system.

1.1.1 Specific Aim 1

The first aim is to design and identify the right electrode system based on the size, area, and sensitivity. Various electrode designs are constructed, fabricated and are studied to determine the best performing electrode design for the desired sensor application. A portable field based sensor needs to utilize and leverage small volumes of plant sap to enable effective and optimal detection of the target biomolecule. The sensors designed for this aim are on hard substrates, such as glass

or on a printed circuit board (PCB) to make them portable and easy to use under all conditions. This aim will focus on the design considerations needed to be taken to produce a sensor with a high level of consistency and low sensor to sensor variability and with consistent baseline measurements while running electrochemical impedance spectroscopy studies.

1.1.2 Specific Aim 2-A

The second specific aim focuses on the construction of an affinity based immunoassay to facilitate bio-sensing, after identifying the sensor that is designed in the first aim. The second aim focuses on achieving independent characterization of each of the above identified viruses in a simple buffer medium namely Phosphate Buffer Saline (PBS). A dose dependent response is also recorded to determine the sensitivity of the system. The aim is mainly designed to show proof of concept and the successful detection of the target bio-molecule before moving onto the complex medium of its existence, namely plant sap. Various sensor parameters such as limit of detection, limit of blank, sensitivity and dynamic range are determined in this specific aim.

1.1.3 Specific Aim 2-B

In the final aim, the focus is to independently characterize and detect each of the target bio-molecules in a complex buffer media namely plant sap. An immunoassay is constructed for the detection of plant pathogen in plant sap. The immunoassay is improved based on the results achieved in aim 2-A of this work. The aim is designed to depict the successful detection of the target bio-molecule in the complex medium of its existence. A dose dependent response is also recorded to determine the sensitivity of the system and other sensor parameters such as limit of detection, limit of blank, and dynamic range are determined in this specific aim.

1.2 Motivation

Wheat derives its name from Old English hwæte of Germanic origins; related to Dutch weit, and German Weizen. Wheat is a grass which is majorly cultivated for its seed, a cereal grain which is a staple food worldwide [1] [2] [3].

The first known to be cultivated in 9600 BCE, in the regions of Fertile Crescent (also known as the cradle of civilization), consists of parts of arid and semi-arid regions of Western Asia, Nice Valley, and Nile Delta or most widely used historian term for the region "Mesopotamia" [4] [5].

Since its origin, Wheat, as of 2016, is the second most-produced cereal after Maize. It stands at the fore-front of land area usage, measuring up to 220.4 million hectors worldwide in 2014 with an annual production of 729 million metric tons [6].

Widely used in the food and beverage industry, it is a staple food for many countries worldwide. Its major usage in F&B Industry, is in the production of bread, porridge, biscuits, pancakes, beer, vodka, gin and whiskey.

In 2016, world production of wheat was 749 million tons, making it the second most-produced cereal after maize [7] [8]. In the United States, wheat production is majorly classified into five major classes namely, hard red winter, hard red spring, soft red winter, durum and white. Each of these classes have varied usage and different end products. Majority of the wheat production is concentrated in two of the above classes; hard red winter and red spring wheat.

As per USDA, in a report published in 1998, average operating costs per bushel was $1.43 and total cost per bushel was averaged at $3.97. The study also concluded by stating the average yield per acre 41.7 bushels [9].

Wheat is truly a global commodity, given its wide usage. The wheat commodities are very volatile with changes in prices typically ranging from 0.5-5%. When the wheat prices are high, the companies generally tend to take a hit on their gross margins and/or they pass the cost differences to the consumers. America exports 50% of its produced wheat to foreign countries [10].

With the production of wheat comes associated losses. Large wheat grain producing nations report loss of yield due to a number of factors such as poor storage technologies, diseases, natural calamities and lack of supply chain. Yield losses only due to diseases caused by pathogens, animals and weeds are reported to be ranging between 20 and 40% of global agriculture productivity [11]. The phrase “losses between 20 and 40 %” therefore inadequately reflects the true costs of crop losses to consumers, public health, societies, environments, economic fabrics and farmers [12]. More than 800 million people do not have adequate food; 1.3 billion live on less than $1 a day and at least 10% of global food production is lost to plant disease [13] [14] in the United States, it is estimated that there is a loss of 1 million tons of wheat per year valued at 35million dollars, just due to wheat viral diseases [10].

With having established the importance of wheat in all the industries, especially in the food and beverage industry, it is important to try to protect and preserve the wheat grown all over the world, to increase yield, reduce losses, increase productivity and more importantly, to address the global food situation of hunger and starvation.

1.3 Innovation

There is rapid growth and use of affinity based sensors in the human world to diagnose various diseases and conditions. The agriculture realm, lacks a device that is portable, robust, and provides diagnosis of a disease within a few minutes. Current technology, such as ELISA, PCR and dot blotting either requires expensive equipment, takes a long time to produce results, or both. The agriculture industry, just like the human industry deserves excellent care and top-notch diagnosis and treatment options.

The innovation of this work comes from the need to develop a field based sensor for the multiplexed detection of plant pathogen for the early identification of diseases that affect crops and cause loss in revenue on a large scale. The development of this kind of sensor coupled with a portable potentiostat, will be the first field based biosensor of its kind.

By making use of electrochemical studies such as EIS, combined with a suitable immunoassay protocol, an affinity based biosensor is developed for the real-time, field based detection of plant pathogen.

CHAPTER 2

BACKGROUND

2.1 Wheat

Wheat was briefly introduced in the first chapter of this thesis to state the significance for choosing wheat and its associated wheat viruses to present the work conducted in this research. Wheat is grown all over the world and as of 2016, is the second most-produced cereal after Maize. It stands at the fore-front of land area usage, measuring up to 220.4 million hectares worldwide in 2014, with an annual production of 729 million metric tons.

The growth of wheat is aided by technological advances in soil preparation and seed placement at the time of planting. Use of crop rotation and fertilizers, and advances in harvesting methods have combined to improve the quality of yield. All these factors, promotes wheat as a viable crop.

Wheat has a high adaptability to varied weather conditions and can be grown in tropical and sub-tropical conditions. It can tolerate severe cold and snow; and can resume its growth cycle during the spring season in warmer conditions. Although, the ideal conditions to germinate the wheat seed is 20-25 degrees Celsius, the seeds can be germinated in temperatures ranging from 4-35 degrees Celsius. Altitude is not a big constraint either, as it can be grown from sea level to as high as 3000 meters.

Wheat is grown in diverse types of soil, ranging from desert soil to heavy clay soil. Ideally wheat is grown in a well-drained, fertile clay loam soil having moderate water holding capacity and heavy soils with open structure which can retain the monsoon rainfall for longer periods.

According to University of Minnesota, “when diseases and other crop pests are not limiting, average yields continue to increase slowly with time. Adequate and efficient use of fertilizer has been a major contributor to this increase”. An average wheat grower receives more yield or return by nitrogen usage than any other nutrient since wheat is very sensitive to insufficient nitrogen. Placement and time of application of nitrogen fertilizers have varied effects on yield. Some methods of application include – drilling in with the seed, sideband placement, banding into soil prior to seeding etc. Drilling in with the seed has proven to be the most effective and widely used method.

Wheat is widely used in the food and beverage industry, it is a staple food for many countries worldwide. Its major usage in F&B Industry, is in the production of bread, porridge, biscuits, pancakes, beer, vodka, gin and whiskey in no particular order.

In the United States, wheat production is majorly classified into five major classes namely, hard red winter, hard red spring, soft red winter, durum and white. Each of these classes have varied usage and different end products. Majority of the wheat production is concentrated in two of the above classes; hard red winter and red spring wheat. The following table (2.1) depicts the usage, primary production regions, quantities of wheat produced in the United States:

Table 2.1: Summary of production, location and usage of wheat grain in the United States [15]

Class	**2011 Production (in bushels)**	**Location Produced**	**Usage**
Hard Red Winter	780 million	Great Plains (TX to MT)	Bread flour

Hard Red Spring	398 million	Northern Plains (ND, MT, MN, SD)	High-protein blending
Soft Red Winter	458 million	Eastern States	Cakes, cookies, crackers
White	314 million	WA, OR, ID, MI, NY	Flour for noodles, crackers, cereals
Durum	50 million	ND, MT	Pasta

The harvested wheat grain which enters trade is classified and graded according its properties and usage. Buyers use these classifications to decide which wheat to buy and which will be more profitable with constraints on the seasonality, yield, location and farm sizes.

As per USDA, in a report published in 1998, average operating costs per bushel was $1.43 and total cost per bushel was averaged at $3.97. The study also concluded by stating the average yield per acre 41.7 bushels.

The most important trading venues for wheat are the London International Financial Futures and Options Exchange, the Chicago board of Trade, the Kansas City Board of Trade, and the Minneapolis Grain Exchange. Some notable major players/ buyers of wheat in the commodities include, Kellogg, General Mills, Kraft Foods, PepsiCo, and Nestle.

Wheat is truly a global commodity, given its wide usage. The wheat commodities are very volatile with changes in prices typically ranging from 0.5-5%. When the wheat prices are high, the companies generally tend to take a hit on their gross margins and/or they pass the cost

Figure 2.1: Dollar price per bushel 1997-2017 [54]

differences to the consumers.

The rise in the price of wheat on the turn of the century, as shown in figure 2.1, sheds light on how important wheat has become in the food and beverage industry. Despite the rise in production, the costs increased as well because of the cost of production and demand. Wheat has become an important part of daily life with wheat being a staple diet for many sets of population and with rice, wheat is the world's most favored staple food. There are 21 known types of wheat grown all over the world, and the reason it is a favorite is because it can be grown even in extreme climatic conditions. All the statistics mentioned sheds light on the significance of choosing wheat virus as the target for the work presented in this thesis.

2.2 Soil Borne Wheat Mosaic Virus (SBWMV)

The first of three plant pathogens picked during the course of this research is a virus that affects wheat, barley and rye cultivars with wheat being the primary host- soil borne wheat mosaic virus (SBWMV) [16]. The disease, often misdiagnosed as a nutritional problem due to the lack in knowledge, spreads very quickly and goes untreated. The figure 2.2 shows the appearance of

Figure 2.2 Crops infected by SBWMV [58]

infected crops at a distance. SBWMV is part of the Furovirus genus, whose members, are characterized by rod shaped particles and positive sense RNA genomes. The RNA genomes comprise two molecules, one of which is used for replication or mobility while the other is used for defense against the host [17]. The virus is vectored by a fungal organism, Polymyxa graminis, whose asexual secondary and sexual primary cycles help the virus spread. The disease causes root cell infection and is a serious contributor to loss in crop yield. It has been reported that the loss lies anywhere between 3% and 85%, depending on the location.

The primary host for SBWMV and the only known host, is the wheat plant, Triticum astivum [18]. These symptoms include leaf mottling, leaf mosaic, stunting, and blotting of the leaves similar to the type seen in wheat spindle streak mosaic virus. The symptoms may range from mild green to yellow, and leaves may sometimes have parallel streaks, reddish streaking, and necrosis at the tips. Symptoms usually occur around the same time each year. This time is usually early spring, although in warmer climates it is possible that symptoms can emerge in late fall or early winter. The virus lasts until early summer and diminish as the temperature increases to 75°F and above.

Temperature and soil moisture immediately after planting are critical factors to how much virus transmission occurs and subsequently, the quality of yield. Traditional farming techniques such as crop rotation is ineffective since the vector, can survive in dry soil without a host for up to 8 years, which means that once the onset of the infection occurs, it is very difficult to prevent the spread, making SBWMV a serious disease.

2.3 Wheat spindle streak virus (WSSMV)

Wheat spindle streak mosaic virus (WSSMV) is also known as yellow mosaic virus. WSSMV is the second target antigen chosen for this work. It was first reported in the 1960's in Ontario, Canada. It was then reported in Kansas in 1984, although it may have entered the United States much earlier.

The symptoms, life cycle and patterns are very similar to the SBWMV discussed in the previous section. The similarity was probably unrecognized until SBWMV was suppressed by treatment against the disease. The similarity lies only in the external morphology, however, the viruses are unrelated.

The symptoms, again are similar to the SBWMV. Usually symptoms of WSSMV appear before SBWMV. The optimum temperature for symptom development is 50°F. Above 64°F new growth will be symptomless, but symptoms may persist on older leaves. The symptoms of WSSMV are yellow to light green streaks or dashes on a dark green background. Dashes are usually 1/8 to 1/4" long. The figure 2.3 shows a picture of the symptoms describing WSSMV.

Figure 2.3: Leaves infected by WSSMV [59]

The dashes observed on the leaves are oriented parallel to the leaf veins and often tapered which gives the lesion a spindle like shape, and hence the name WSSMV. The appearance of the spindle, differs from the SBWMV in the manner that the SBWMV, has islands of green in an overall yellow background. Like WSBMV, the field pattern of WSSMV tends to follow the lower, wetter areas of the field.

Both SBWMV and WSSMV are vectored by the same organism, Polymyxa graminis. The viroid particles are vectored in the fungal zoospores. The fugus affects and infects the root hair of the young wheat plant. The fungus forms dark clusters of resting spores in the wheat roots which are released to the soil when the roots decay. Since the fungus survives in the soil as resting spores, the disease is always associated with infested soil. Soils may remain infective for at least 8 years. Neither WSSMV or SBWMV are vectored by insects or in seeds. losses caused by WSSMV are difficult to measure. They are dependent both on the cultivar and the weather [19].

2.4 High Plains Virus (HPV)

The third and final choice of target antigen, is the high plains virus (HPV). HPV was first reported in Kansas in 1993, making it a relatively new virus. It may have been around for while, however, it was never reported or discovered. The virus particles appeared similar to those in the tenuvirus group and hence was names the high plains tenuvirus, or simply, HPV.

The virus is seen to be found in both corn and wheat [20]. It is vectored by wheat curl mite, Acerica tosichella, which is the only known host [21] [22].

Symptoms include stunting, yellowing and strong mosaic. Plants affected by HPV have a distinctive longitudinal red stripe along the lamina of the leaf. It is found that WSSMV is a common infection that is coupled with HPV, which means that SBWMV is also associated with this disease. Symptoms of pure HPV infection are quite variable. Some leaves have green and yellow stripes at the leaf tips similar to wheat streak mosaic. Others have yellow spots. Still others have green islands on a light green background and look similar to SBWMV.

Wheat, barley, some varieties of oats, some varieties of corn, downy brome, green foxtail, and yellow foxtail are confirmed hosts of HPV. Curl mites can multiply on all of these hosts, so some

of these could possibly be a source of HPV [23]. Mites depend on wind to help them spread to unaffected plants. They are unaffected by cold temperatures and can survive the winter, however, their only weakness being, the need for fresh plant material, without which they survive only up to 10 days.

The amount of loss contributed by HPV seems to be relatively unknown, since it is a relatively new virus to have been discovered.

The three pathogens are seen to be commonly associated with each other in terms of their symptoms, disease cycles, and time of appearance and the type of crops they affect. Therefore, the three diseases, SBWMV, WSSMV, and HPV are the three viruses chosen for the study conducted in this thesis.

2.5 Current wheat pathogen detection techniques

Having discussed the three target antigens for the scope of this project, the current technologies used to detect the three molecules of interest are assessed and evaluated. The three main techniques used in detecting and diagnosing the wheat plants are 1) Enzyme linked immunosorbent assay (ELISA); 2) Polymerase chain reaction (PCR); 3) Dot blots.

2.5.1 Enzyme linked immunosorbent assay (ELISA)

ELISA is a popular form of analytic biochemistry assay that uses a solid phase enzyme immunoassay to detect the presence of a target antigen suspended in a sample. It is a test that uses color change to identify the presence or absence of a substance. ELISA has been used as an accurate diagnostic tool in medicine and plant pathology as well as quality control check in various industries. There are various types of ELISA that can be done to achieve analyte

detection. Enzymatic immunoassays are broadly categorized into two headings, namely homogeneous and heterogenous immunoassay [24]. The types of ELISA used depends on the target analyte in question. The main types of ELISA are direct ELISA, indirect ELISA, sandwich ELISA, competitive ELISA [25].

ELISA studies conducted on the three antigens procured, involves using a direct ELISA. Direct ELISA is a technique suitable to determine the presence of antigens that have high molecular weight. Figure 2.4 summarizes the direct ELSIA process. In this process, the surface of the plate is coated directly with the antibody or antigen. An enzyme that is tagged with this antibody or antigen enables the measurement. Incubation is followed by washing which removes the unbound antigen. The appropriate substrate is added to the medium to produce a signal through coloration, the signal is then measured to determine the amount of antigen or antibody [26].

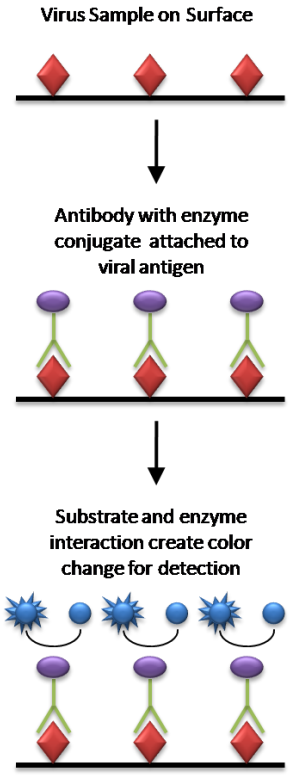

Figure 2.4: Direct ELISA Diagram [57]

ELISA has a number of advantages, it is accurate, has low sensitivity, no expensive laboratory equipment is required. It does have its fair share of disadvantages of being non-portable, requirement of multiple reagents, and most importantly, it is time consuming and cannot produce rapid results.

2.5.2 Polymerase Chain Reaction

This is a technique used in molecular biology to amplify a few copies of a segment of DNA across several orders of magnitude. It is an easy, cheap and reliable method to replicate a focused DNA segment, which is a concept that can be applied to several fields in modern sciences. It is used in DNA cloning, gene cloning, monitoring of hereditary diseases, amplification of ancient DNA and many other applications.

The PCR process relies on a process called thermal cycling, where there are multiple heat-cool cycles, which allow a range of temperature dependent reactions such DNA melting, and enzyme based DNA replication. The DNA generated in PCR serves as its own template for making several copies of the generated DNA sequence, after the complementary primer, to the original sequence is input along with DNA polymerase.

The PCR process contains a series of repeated temperature changes, ranging between 20 and 40 changes, called cycles. Each cycle contains three discreet steps, denaturation of the DNA sequence, annealing, and elongation.

The first PCR step is initialization- this step is required for the DNA polymerase which requires heat activation. The next step is the denaturation of the DNA sequence, by a process called DNA melting to split the helix into two single strands. The next step is to anneal the sample to the right

temperature to allow the DNA to hybridize. The final step is elongation, wherein the DNA polymerase now synthesizes new DNA molecules. There is a final elongation step which is optional. To check if PCR was successful, the products of the PCR are segregated by size using gel electrophoresis and then matching the size to a DNA ladder, which serves as a reference sheet. The schematic of PCR is shown in the figure 2.5.

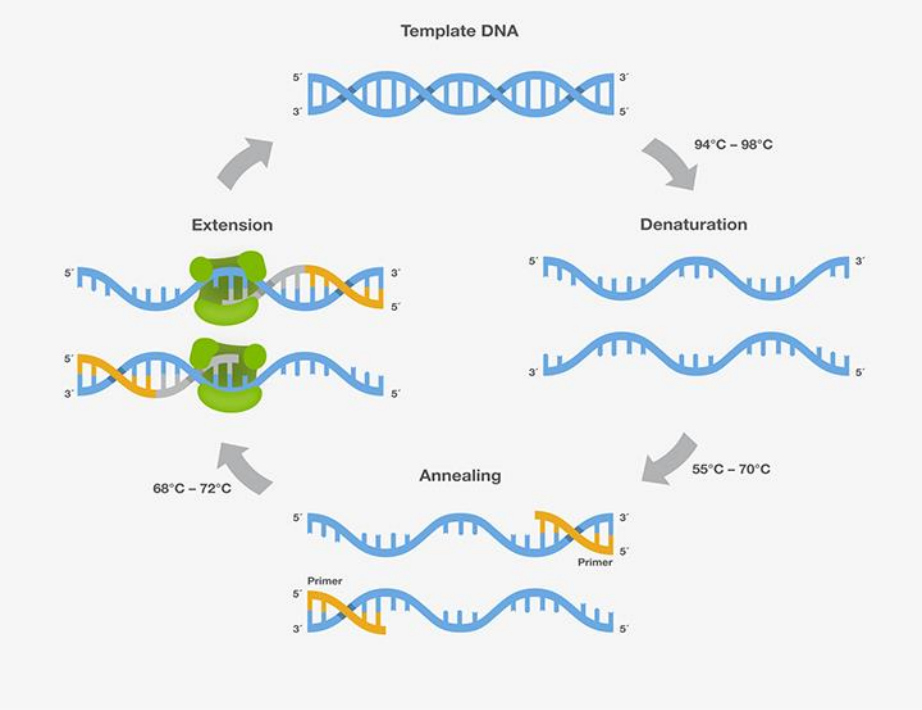

Figure 2.5: Schematic of polymerase chain reaction [60]

PCR allows for the rapid and accurate diagnosis of infectious diseases caused by bacteria or viruses [27]. The basis for PCR diagnostic applications in microbiology is the detection of infectious agents and the discrimination of non-pathogenic from pathogenic strains by virtue of specific genes [28].

PCR has several advantages. It is simple to use, and produces results rapidly. It is highly sensitive and can produce multiple copies of the target DNA from a single strand and can be quantified successfully. It is repeatable and therefore economical.

Some limitations include, the requirement of prior knowledge of the target sequence. Secondly, it is prone to error even if a small detail is mismatched in the sequencing which is capable of causing mutations in the generated PCR products. Further, it is non-portable and therefore needs use of specialized bench top equipment.

2.5.3 Dot blots

Dot blotting is a technique used in molecular biology to detect biomolecules. It represents a summarized method of various blotting techniques, such as northern, southern and western blots. In a dot blot, the antibody whose biomolecule is to be detected is immobilized on a specific type of membrane. The physiological fluid in which the target molecule is suspended is added to the membrane. The membrane is the subject to electrophoresis after which a stained band is generated on the blot.

Polyacrylamide gel is generally used for the electrophoretic separation of proteins, and SDS is generally used as a buffer (as well as in the gel) in order to give all proteins, present a uniform negative charge, since proteins can be positively, negatively, or neutrally charged. This type of electrophoresis is known as SDS-PAGE (SDS-polyacrylamide gel electrophoresis). Prior to electrophoresis, protein samples are often boiled to denature the proteins present. This ensures that proteins are separated based on size and prevents proteases (enzymes that break down proteins) from degrading samples. Following electrophoretic separation, the proteins are transferred to a membrane, where they are blocked, to prevent non-specific antibody binding and

finally stained with antibodies specific to the target protein [29] [30]. Lastly, the membrane will be stained with a secondary antibody that recognizes the first antibody staining, which can then be used for detection by a variety of methods.

Dot blots are inexpensive, do not require expensive laboratory equipment, and are fairly accurate for concentrations of analyte in the 100's of microgram/mL region. However, they have a certain number of disadvantages as well. They are non-portable, require a number of reagents and benchtop laboratory equipment which would mean that it is non-portable. Results are not rapid and do take time.

2.6 Electrochemical Impedance Spectroscopy

From the principles of Ohm's law that resistance is defined as the obstruction to the flow of current. This is a simplified definition and only applies to direct currents (DC) and does not hold good for alternating currents(AC). For AC the resistance is a complex element, comprising of real and imaginary parts due to the electromagnetic nature of a signal in an AC circuit. Electrical impedance is defined as the ratio of change in voltage, to the change in current.

Impedance spectroscopy refers to a technique wherein, a constant AC voltage is applied and the corresponding current is recorded to estimate the impedance. The process is repeated for a range of frequencies and each frequency has a corresponding value of impedance.

Electrochemical impedance spectroscopy (EIS) is a technique that uses impedance as a reporting metric by looking at change in electrical properties of a system [31]. EIS works by applying a sinusoidal voltage across an electrochemical cell, which is a two-electrode system biosensor. When a potential is applied to the electrode, it becomes polarized and becomes charged.

Consequently, it attracts oppositely charged particles to its surface and forms a double layer called electrical double layer (EDL).

In this case an AC signal of 10mV amplitude is applied. The resulting current is measured for each frequency step and the impedance is calculated. The impedance can be calculated by evaluating the resulting current and phase shift in the signal [32].

EIS results, are typically fit into an equivalent circuit model containing passive electrical circuit components. The most commonly used model, Randles cell, shown in the figure 2.6, [33] consists of a capacitor, two resistors, a constant phase element, and a Warburg impedance. The first resistor (R_s) describes the solution resistance which occurs due to effects in the bulk of the solution and not due to phenomena occurring at the electrical double layer. In the parallel branch of the circuit, the R_{ct} describes the charge transfer resistance- dominant in faradaic biosensors, describes the resistance due to electron transfer between the electrodes and the redox molecule of the electroactive species; C_{dl} describes the double layer capacitance, which occurs due to changes in the properties of the double layer; Z_w depicts Warburg impedance- significant in faradaic biosensors, is a resultant of the diffusion in the ions caused in the solution. The main components that are studied in bio-sensing are the R_{ct} and C_{dl}. The whole circuit is representative of the electrical double layer that is formed on the surface of the electrode.

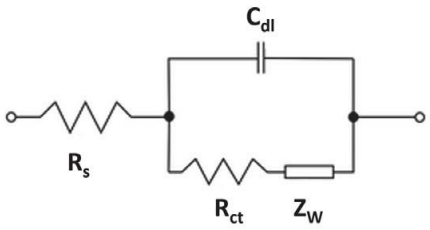

Figure 2.6: Randles Circuit [33]

Impedance based biosensors rely on the capacitive components of the circuit for sensing. For the work presented in this thesis a two-electrode system (non-faradaic system) is used and therefore the primary focus is to evaluate the changes in the double layer. Since the focus lies in the evaluation of the modifications occurring at the electrical double layer (EDL) we look at changes specifically in the capacitive element C_{dl}, which is the component of interest, using EIS [34] [35]. As the immunoassay is built, which is discussed in later chapters, each stage of the immunoassay will all have properties that modulate the electrical double layer, both in thickness and in the electrical permittivity, which will be reflected in the impedance response of the system. The responses at each step, obtained from EIS data, will be used to evaluate the system.

2.7 Electrical Double layer

The electrical double layer is formed when an ionic fluid comes in contact with a polarized electrode. In the case of biosensor applications, the ionic fluid is a physiologically relevant fluid, which is chosen based on the desired target biomolecule. The electrical double layer consists of three main layers. The first layer, is the surface charge of the electrode surface, which is polarized and causes ions to be adsorbed on the surface due to the chemical interaction that takes place. The second layer is a layer of opposite charges attracted by the electrostatic force that exists between oppositely charged particles. This is known as the stern layer. The double layer formed on the surface essentially behaves as a parallel plate capacitor and hence has a surface capacitance associated with it. The capacitance is given by the equation:

$$C = \frac{\varepsilon_o \, x \, \varepsilon_r \, x \, A}{d}$$

Where ε_o is the absolute permittivity of the system, ε_r is the relative permittivity of the system, A is the area between the "parallel plates" corresponding to the area of the EDL and d is the thickness of the EDL.

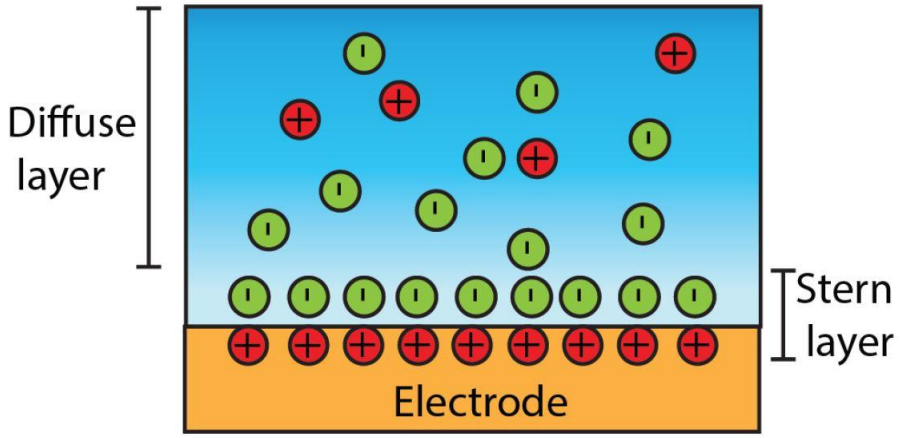

Figure 2.7: Schematic representation of electric double layer

The ionic charge distribution formed further from the double layer due to the influence of the electric field is called the diffuse region. The characteristic length of the double layer formed due to the electric field is then called the Debye length. As the properties of the double layer (length, thickness, permittivity) are modified, the surface capacitance changes and thereby the overall impedance of the system also changes. The double layer is modified when there is a modification of the electrode surface, which occurs during the construction of the immunoassay. A schematic representation of the EDL is presented in the figure 2.7.

2.8 Biosensors-review

Biosensors are devices that detect the presence of any kind of biomolecule, through the use of a sensing site or a recognition site, a signal transducer that converts the obtained bio-signal into a

meaningful form, and some kind of output element to help interpret the results obtained. Since bio-signals are very weak in nature, it has to be amplified to bring it to a measurable value, and therefore goes through a signal amplifier. The data once acquired, may need post processing and cleaning to make sure that the data obtained conveys some useful information.

Many biosensors are affinity based, which means that they use an immobilized capture probe, which is at the sensing region, to capture the target molecule to be sensed, that is the target analyte [36].

There at multiple ways to detect this signal that is localized at a surface. One such method is the use of electrical biosensors that rely on current or voltage measurements to detect binding [37] [38] [39]. Other sensors include sensors that use light, such as surface plasmon resonance, fluorescence, sensors that use mechanical motion- quartz crystal microbalance and others that use magnetic particles to detect the target molecules. Due to their low cost, electrical biosensors have great promise for applications where minimizing the size and cost is crucial. Electrical biosensors can be further subdivided according to how the electrical measurement is made, including voltammetric, amperometric/coulometric, and impedance sensors. We choose impedance sensors by using EIS which is discussed in the previous section of this thesis.

Having discussed the earlier techniques, its advantages and drawbacks, the need for an affinity based biosensor can be seen. Some of the advantages that comes with affinity based biosensors are, 1) Inexpensive; 2) rapid results; 3) high sensitivity; 4) high specificity. Having stated the need, a biosensor is now developed towards the multiplexed sensing of plant pathogen in plant sap, or what will be referred to as “SapSense”.

CHAPTER 3

MATERIALS AND METHODS

3.1 Printed Circuit Board (PCB) Substrate

The electrode system used, is deposited on a PCB substrate, manufactured by PCB universe. The PCB comprised of two basic parts, namely, a substrate and a layer of the printed electrode. The electrode material used is gold. The purpose of the substrate is that it physically holds the circuit components and provides electrical insulation between the conductive parts. The type of substrate used is FR-4, a fiberglass-epoxy laminate, which is similar to the other fiberglass boards. Additionally, the FR-4 is flame resistant. The FR-4 material is rigid and strong, and are usually found in high quality electronics.

3.2 Sensor Setup

The figure 3.1 shows the fabricated biosensor device, which consists of two components, the substrate and the gold microelectrode fabricated on a FR-4 printed circuit board. The spacing between the microelectrodes was maintained at 2mm. The microfluidic encapsulant layer was made up of PDMS. The microfluidic chamber was designed to position the desired buffer over the printed electrode surface.

The PCB was initially cleaned to remove organic contaminants using isopropyl alcohol (sigma Aldrich, MO, USA) and de-ionized water. The polydimethyl siloxane (PDMS) encapsulant designed to hold the sample has a single provision for injection and withdrawal of fluid onto and from the sensor platform. The PDMS was prepared using a Silicone 184 elastomer kit (Dow Corning, MI, USA). The kit consists of two parts namely the elastomer base and a curing agent

which are mixed in the ratio of 10 :1 respectively. The mixture of the base and the curing agent was poured into an aluminum mold and heat cured for one hour at 100 C by placing the mold on a hot-plate. The PDMS was then fastened onto the PCB substrate using a water proof silicone sealant. The PDMS encapsulant holds a volume of up to 40µL which formed the volume sample size for all experiments.

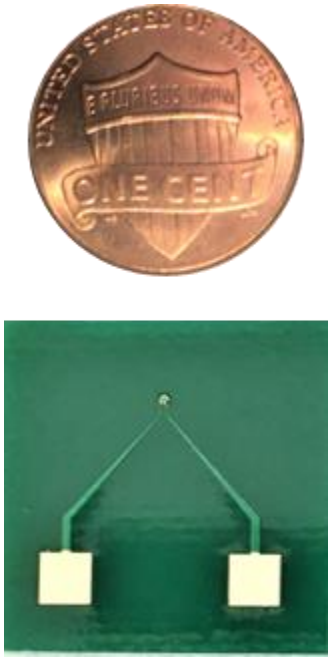

Figure 3.1: Two electrode system- sensor setup

The dimension of the sample chamber about 4mm in diameter and about 2 mm in height. The total volume the chamber could hold was about 20µL. The integration of the microfluidic chamber and the PCB is performed using a water proof silicone sealant to ensure biocompatibility and non-reactivity.

The overall dimension of this device is about 2 cm by 2cm. The two terminals of the electrodes, namely the working and the counter and the reference are then connected to the potentiostat which is used to perform electro impedance spectroscopy on the desired sample. The connections

to the potentiostat are made using solder leads and copper wires to ensure that there is minimal or no voltage drop occurring during the transmission of the voltage signal from the potentiostat to the sensor.

3.3 Sensor Design and Optimization

The electrode geometry plays an important role in determining the effective signal transduced as a result of change in the surface properties of electrodes, which was previously touched upon in specific aim 1. There are four types of electrodes studied for the application discussed in this dissertation, of which one electrode design is finally used for the detection and quantification of plant pathogen in plant sap. The system uses a two-electrode system, comprising of the working electrode and the reference electrode, to which an AC signal is applied. When a buffer solution or any biological sample is added to the sensing area, the constituents modulate the flow of electric charges, which are correlated to the impedance changes that is measured.

3.3.1 Design Version 1

The first design is a two-electrode system. The design consists of 1 reference/counter electrode and three working electrodes. The three working electrodes and a common reference electrode facilitates the sensing of three different biomarkers on the surface of the electrode, functionalized separately making it a multiplexed sensor. A multiplexed sensor is one in which multiple samples can be studied on a single sensor surface. The electrodes are all rectangular shaped with rounded or soft edges to prevent the accumulation of charges along the edges. The ratio of the surface area of the working electrode is maintained at 1:5 with respect to the counter/reference electrode to facilitate easy charge transfer from the working to the reference. The ratio of the

surface areas can be modified based on the application for which it is being used and the required level of sensitivity and specificity. The figure 3.2 shows the design of the sensor.

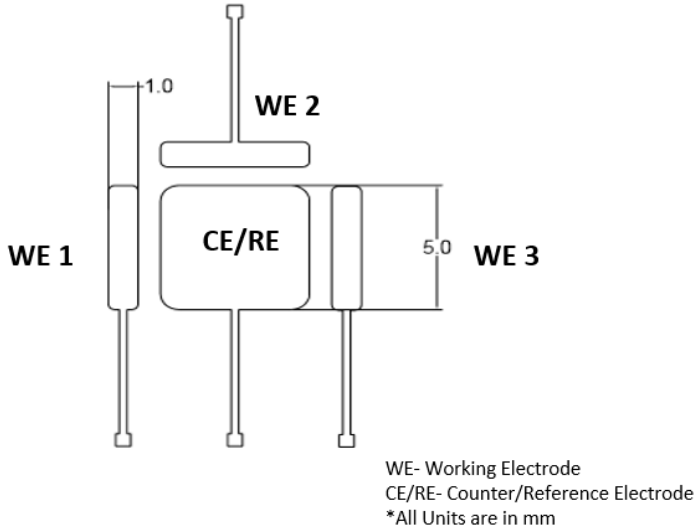

Figure 3.2: Design Version 1

The smallest feature size on this sensor is 1mm, which is the trace of the working electrode. The trace of the reference electrode is 5mm. The trace width of the leads was set at 250µm to ensure the delivery of the AC signal to the electrodes. The working electrodes were set at distance of 1mm from the counter/reference to ensure that fluid functionalized on the working electrode does not leak into the counter/reference electrode. The validity of the sensor design and its feasibility is tested using a simulation software- Comsol Multiphysics. The electrical potential, current distribution and the electric field distribution are simulated with ideal conditions and parameters of the material used for the sensor fabrication. The figures 3.3 and 3.4 show the simulation of electrode design. Electric field is defined as the region around a charged particle in which a force can be exerted on other charged particles. When a test charge is introduced in this

region, a force is exerted on the test charge, either attracting the charges towards the particle or repelling the charge away from the particle depending on its polarity.

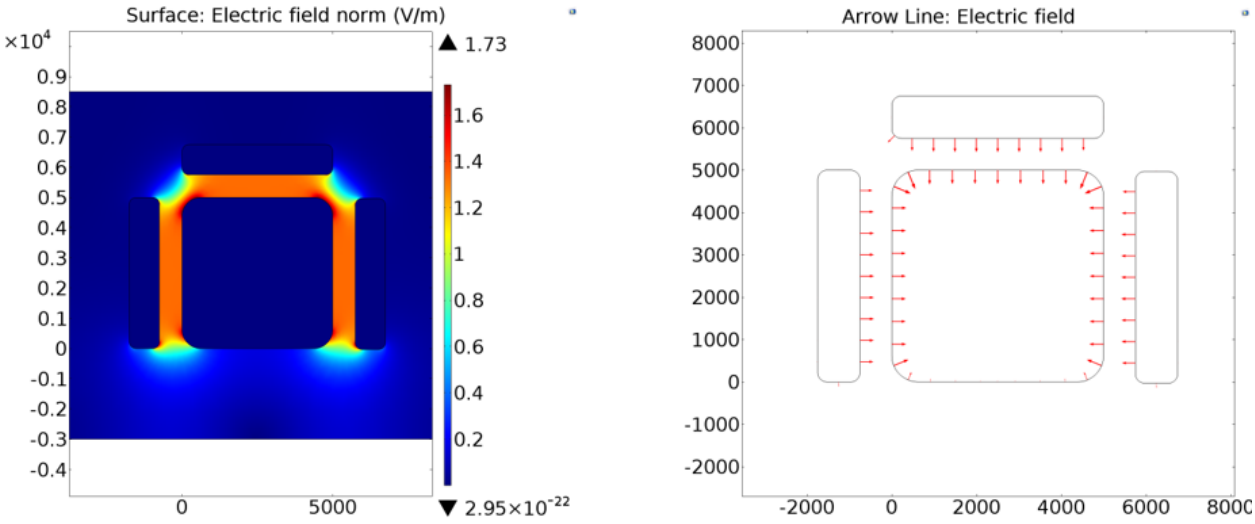

Figure 3.4: Electric field intensity and direction- Design Version 1

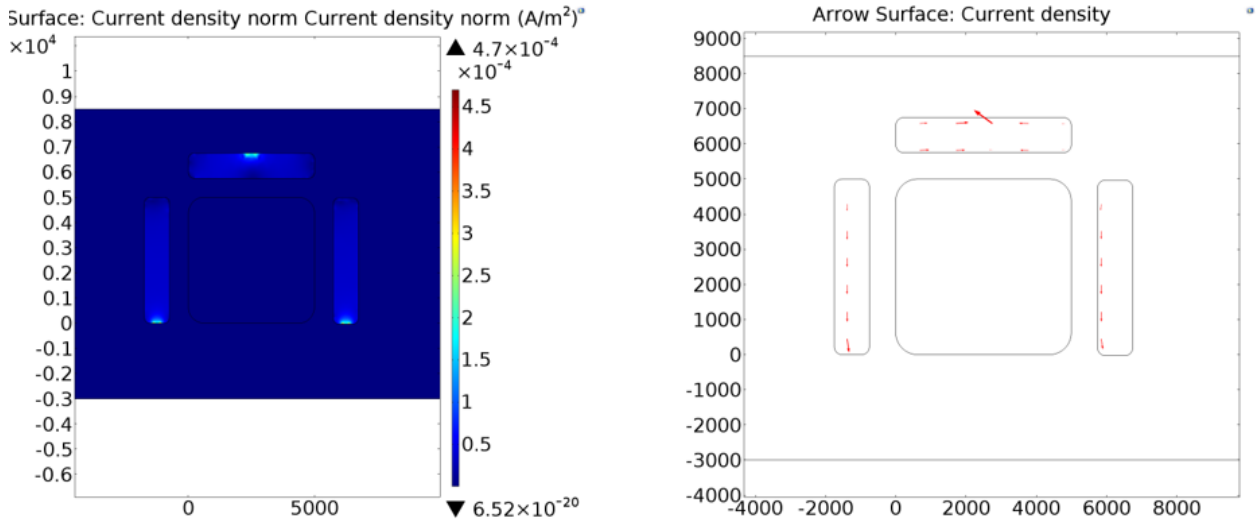

Figure 3.3: Current density distribution and direction- Design version 1

In terms of electrochemistry, the electric field is a region that favors charge transfer between the working electrode and the reference electrode. A strong electric field is indicative of easy charge transfer between the working and the counter/reference electrode and the arrows depict the direction of the flow of the electric field- working to the reference. The current density shows the accumulation of charges at specific regions and from the figure, it is evident that the current is uniformly distributed, which means that any changes that are seen on the electrode surface is due to the modifications in the electrical double layer the electrodes and not due to charge accumulation, which could potentially affect sensing. Secondly, uniform current density would also mean that there will not be localized heating effects due to charge build up in a particular region.

The table 3.1 summarizes all the modelling conditions used for creating the COMSOL models of the electrodes to try and theoretically simulate its behavior when a fixed AC signal is applied to the electrodes when a buffer with known properties is immobilized on the surface of the sensor.

Table 3.1: Summary of modelling conditions used in COMSOL for electrode simulation

Electrical parameter	**Quantitative value**
Electrical resistivity of gold (at 22 Celsius)	2.83×10^{-5}
Electrical conductivity of gold (at 22 Celsius)	4.13×10^{7}
Temperature coefficient (K^{-1})	0.0034
Dielectric permittivity (ε) 6.9	6.9

3.3.2 Design Version 2

Various improvements were required from the Design version 1. Although design 1 was theoretically sound, and had stable baselines, it had some practical issues. For highly hydrophilic substances, it was impossible to contain them on a specific electrode and it was impossible to compartmentalize the electrodes since the distance between the working electrode and counter is indeed small and is about 1mm and thereby selectively functionalize a specific electrode with a specific buffer. Due to the aforementioned drawbacks of design version 1, design version 2 was developed, shown in the figure 3.5.

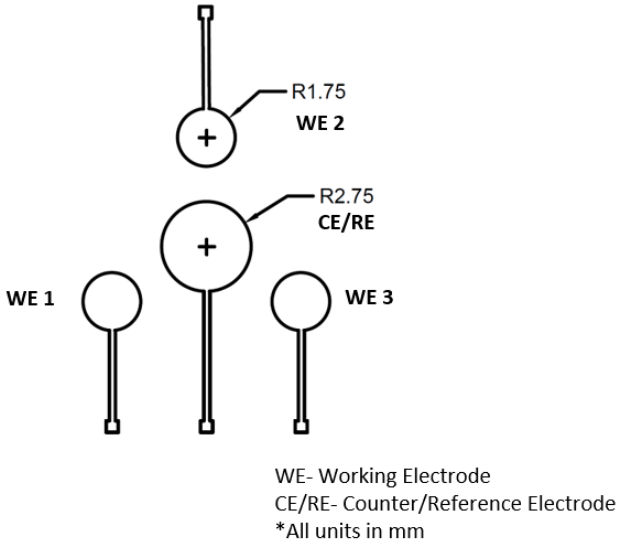

Figure 3.5: Electrode design version 2

This sensor again, is a two-electrode system, with a set of three working electrodes and a common counter/reference electrode. This design is completely different from its predecessor, with the shape of the electrodes being changed to a circle to leverage the surface area is to volume ratio. The smallest feature size for the electrode is 3.25mm which is the working

electrode. The radius of the working electrodes is 1.625mm and the radius of the counter/reference electrode is 2.5mm. The ratio of area of the working electrode is 1:2.4 with respect to the counter electrode. The trace width for the electrode leads is maintained at 0.25mm

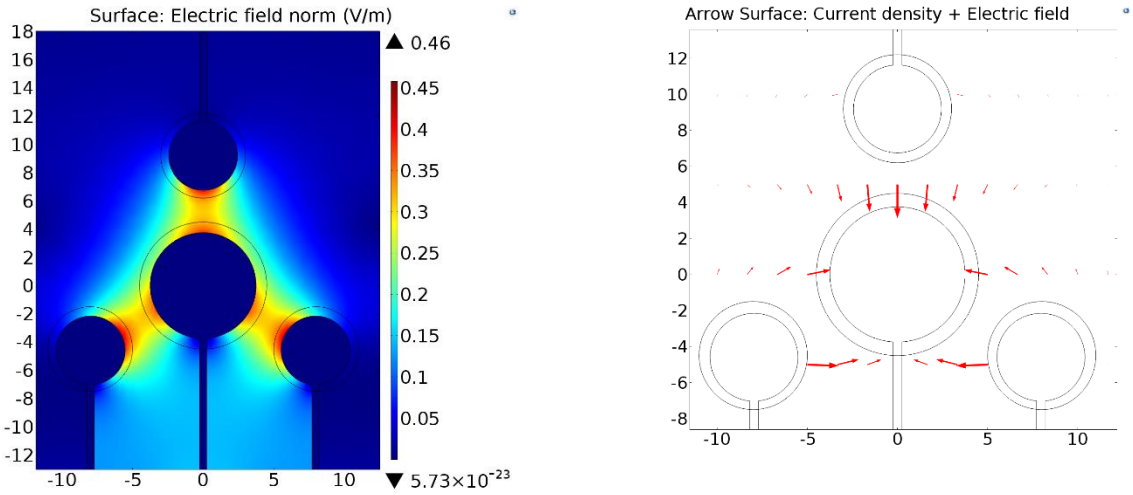

Figure 3.6: Electric field intensity and direction- Design Version 2

for all the electrodes. All the working electrodes are placed at a distance of 2.5mm from the counter/reference electrode, which is much larger than the previous design to prevent the wicking of fluid functionalized on any one electrode onto the reference electrode.

The electrode design was theoretically checked by modelling with COMSOL Multiphysics software. The electrical potential, current distribution and the electric field distribution are simulated (shown in figure 3.6 and figure 3.7) with ideal conditions and parameters of the material used for the sensor fabrication as discussed in table 3.1. The strong electric fields between the three working electrodes and the reference electrode is a desirable characteristic and uniform current density observed on simulation verify that there are minimal areas of charge accumulation and the soundness of the electrode design.

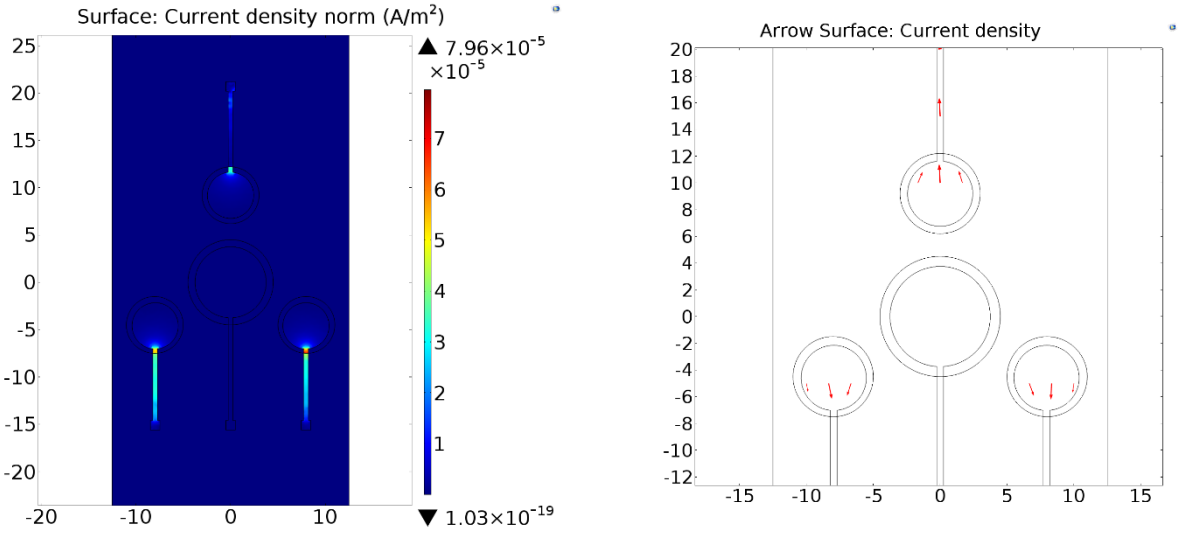

Figure 3.7: Current density distribution and direction- Design Version 2

3.3.3 Design Version 3

Concentrated electric fields around the edges are a common in the electrode designs, due to the accumulation of charges along the edge boundaries. The constant polarization and depolarization of the electrode gives rise to edge effects can affect the sensor structurally and affect the biological sample as well. This is caused due to sharp edges seen in the previous electrode design

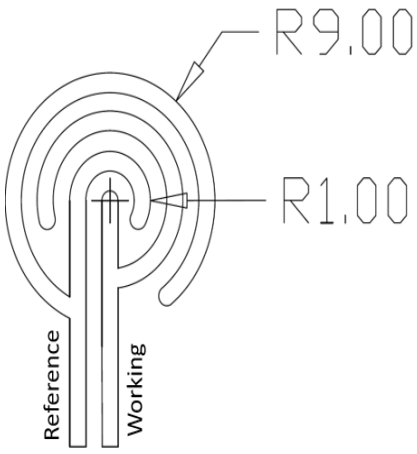

Figure 3.8: Electrode design- Version 3

seen in this dissertation. To overcome this problem, an electrode with fewer edges is constructed with a concentric electrode pattern. The concentric interdigitated electrode pattern, as shown in the figure 3.8, reduces the edge effects significantly, and thereby becomes favorable for bio-sensing. Another useful feature that favors bio-sensing is the use of unequal surface area between the working and the counter electrode. The use of unequal area aids for easy charge transfer from the working electrode to the reference electrode. The ratio of the surface area of the counter to the working is recommended to be greater than a 2:1 ratio. The electrode surface area and the ratio is adjusted based on the application it is intended to be used in. The electrode design shown in the figure 3.8 has a PCB substrate which is patterned with concentric gold electrodes with a trace width of 1mm and an inter circular separation of 1mm [40] [41].

The design is again completely different from version 2, as the multiplexed electrode is now converted to a standalone set of electrodes on a PCB substrate. The multiplexed design was again rejected as it was practically unstable. There was a significant variation for baseline readings from electrode to electrode which would in turn have variable baselines for the same sample within the same sensor chip. Another reason for discarding the multiplexed designs was the

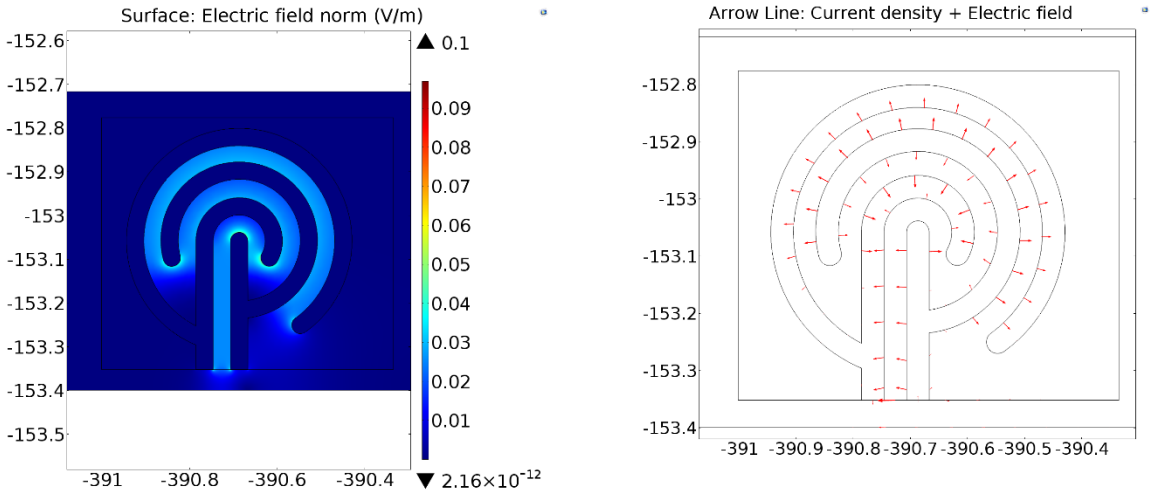

Figure 3.9: Electric field intensity and direction- Design Version 3

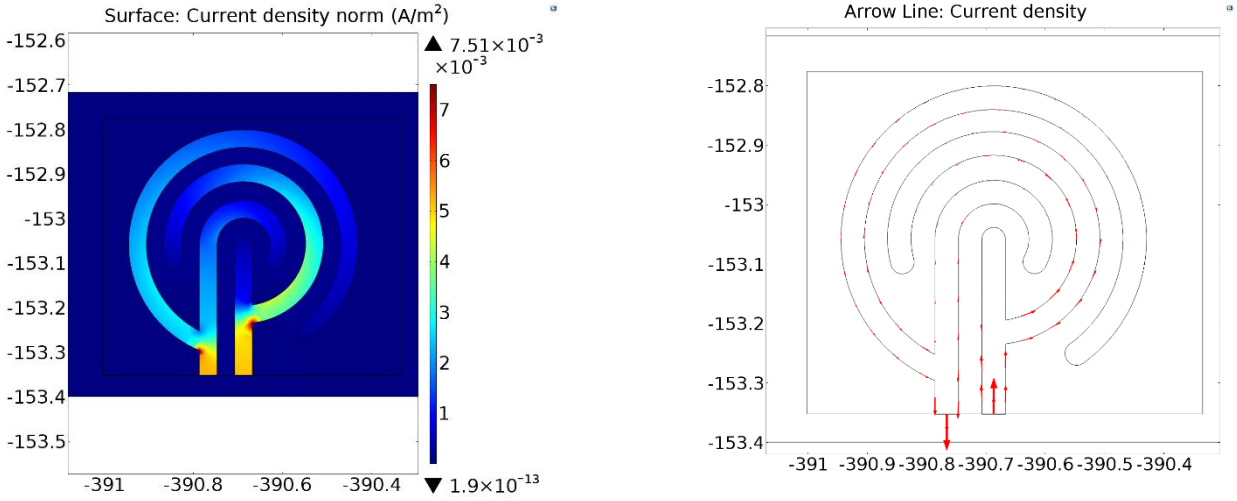

Figure 3.10: Current density distribution and direction- design version 3

presence of cross talk between the electrodes, which could also have contributed to the large variations in the baselines. The design version 3 comprises of one working electrode and one counter/reference electrode. The ratio of the surface area of the working electrode to the surface area of the counter electrode is maintained at 1:10. The design is again simulated theoretically to check the functioning and the feasibility of the design with the results displayed in figure 3.9 and 3.10. The results from the simulation shows a uniform distribution of electric fields, which was one of the aims while making the electrode design. The current density is also uniform and the flow of the charge is observed to be in the direction of the reference/ counter electrode from the working electrode.

3.3.4 Design Version 4

Although design version 3 was a stable in baseline and had a very low chip-to-chip variation in the baseline readings, its only shortcoming was that the impedance values at low frequencies were in the range of thousands of ohm. The application at hand contains very sensitive bio-

molecules which need much higher values of impedances to detect very minute changes at the electrical double layer. In order to achieve this, the fourth design is introduced.

The design consists of one set of electrodes, much like design version 3, with one working electrode and one counter/reference electrode. In order to offset the low impedance values, the size of the electrodes are reduced to a much smaller size, with the trace of the electrodes at 0.05mm and the ratio of the total surface area of the working electrode to the total surface area of the counter electrode equal to 1:2.2. The electrode size/area is exponentially related to the impedance measured. The design is shown in the figure 3.11.

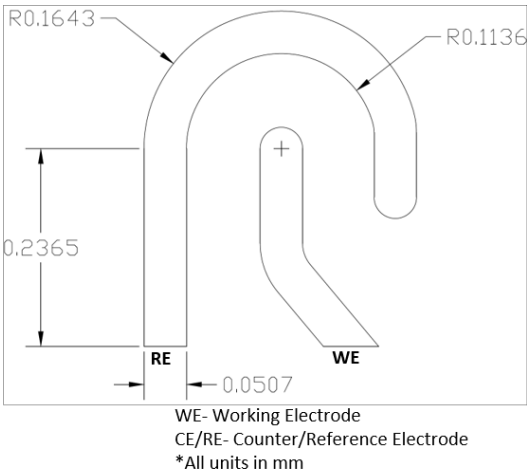

Figure 3.11: Electrode design- Version 4

The design is again simulated theoretically using COMSOL Multiphysics to check the functioning. The results from the simulation shows a uniform distribution of electric fields, which was one of the aims while making the electrode design. A high electric field strength is observed between the working electrode and the reference which facilitates charge transfer. The

current density is also uniform, and the flow of the charge is observed to be in the direction of the reference/ counter electrode from the working electrode.

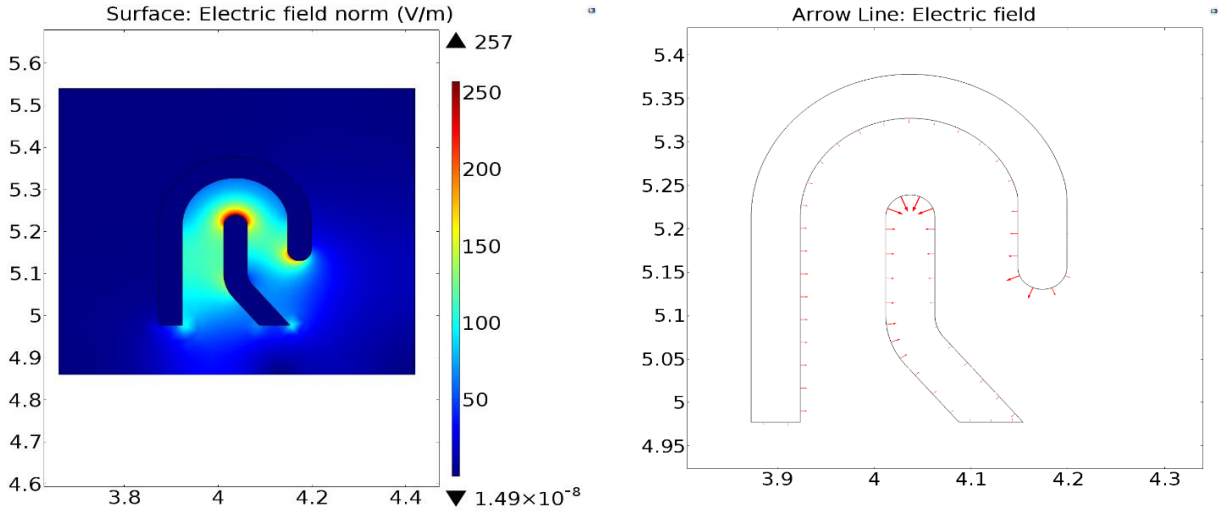

Figure 3.12: Electric field intensity and direction- design version 4

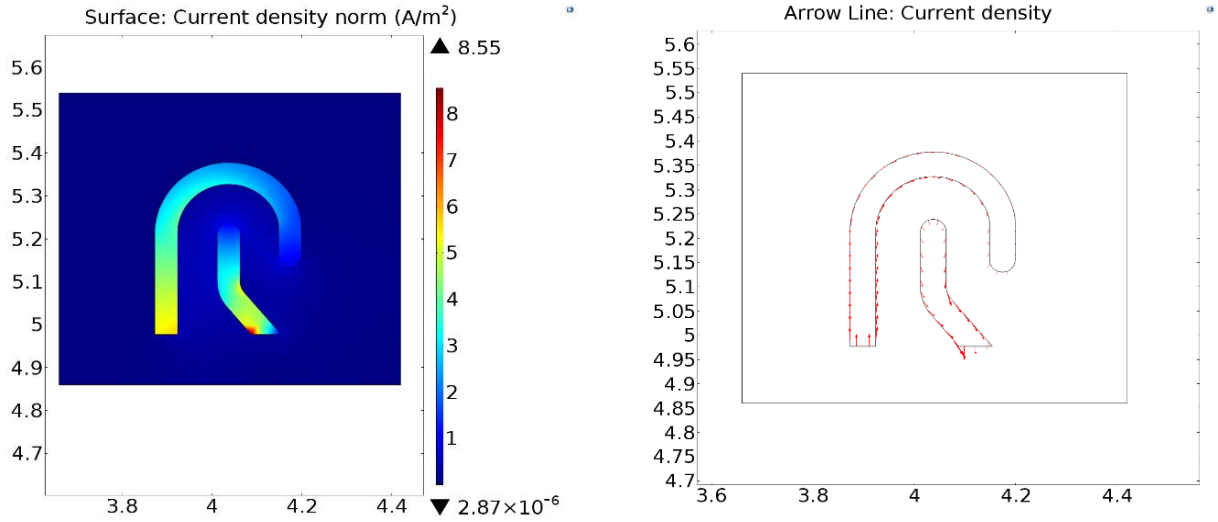

Figure 3.13: Current density distribution and direction- design version 4

The figures 3.12 and 3.13 show the electric field intensities and the current density distribution, respectively, of electrode design version 4. A high current density is observed at certain regions

of the design, due to some of the sharp edges present in this design. The uneven current density distribution seen differs from the more current densities observed in previous design versions. It is higher in certain sections of the sensing region, however, most of the sensing region, has a uniform distribution and is unlikely to affect measurements significantly.

3.4 Buffers, Reagents and Chemicals

3.4.1 Dithiobis (succinimidyl propionate)

A cross-linker is a substance that chemically binds two or more molecules by a covalent or ionic bond. The chemical cross linker of dithiobis (succinimidyl propionate) popularly denoted by DSP is used as the cross linker, wherein the Sulphide ends of the cross linker, binds chemically to the gold [42] electrode while the amine end of the molecule is used to immobilize proteins such as capture antibodies, enzymes among other biomolecules. The structure of DSP as shown in the figure 3.14, contains two N-hydroxysuccinimide (NHS)
ester groups that can react with the primary amine of an antibody to facilitate binding [43]. The NHS esters on either side, are connected to the to a shared disulfide bond. The bond is cleaved in the presence of gold and forms a bond with the gold surface, and subsequently allows the binding of the antibody at the exposed NHS end.

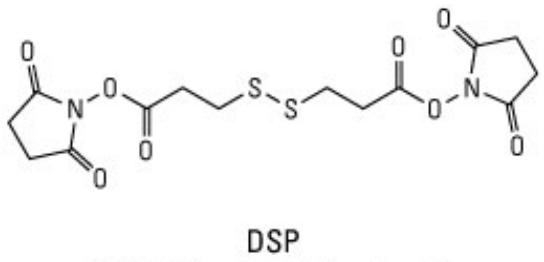

Figure 3.14: Structure-dithiobis (succinimidyl propionate)

3.4.2 Phosphate Buffered Saline (PBS)

Dulbecco's phosphate buffered saline was used to store and dilute the antibody, the plant sap and the three viruses. Phosphate buffered saline (PBS) is an isotonic and non-toxic solution maintained at a neutral pH range between 6.5-7.2. The concentrations used for dilutions and preservation of the various buffers are, 10mM, 1mM and 0.1mM. The buffer contents include monopotassium phosphate, sodium chloride, and potassium chloride and is modified from the traditional mixture to exclude calcium chloride and magnesium chloride. PBS is very popular as it is used for several applications, including cell culture applications, to increase the longevity of stock proteins when used over the course of a few months to years.

3.4.3 Plant Sap

Plant sap, or just sap, is fluid transported in the xylem and phloem cells of a plant. Xylem cells transport water and inorganic nutrients through the plant while phloem cells transport nutrient rich sugary fluids and other biological molecules. Xylem sap is comprised mainly of water, with plant hormones, mineral elements and other nutrients. As water is absorbed from the root of the plants, since the xylem is the main water carrier in plants, xylem-sap moves from roots towards the leaves [44]. Phloem-sap, is made up of manufactured sugars, other biological molecules and mineral elements dissolved in it. Its flow is multidirectional in nature, that is it flows from where carbohydrates are manufactured or stored to where they are used [45]. In the initial growth phases, the roots serve as the sugar sink and later when the plant develops, sugar is produced in the leaves as a product of photosynthesis.

Sap is extracted from the leaves of wheat-grass by grinding the leaves gently using a pestle and mortar. Care is taken not to crush the leaves very hard, since the requirement is just the plant sap and not any other additional proteins or bio-molecules present in the leaf of the wheat-grass. The extracted sap is then mixed with 10mL of PBS buffer, until it produces a clear solution with a green tinge. The solution is then aliquoted into Eppendorf tubes of 1.5mL and is then subjected to centrifugation at 13,000 RPM for a duration of 5-7 minutes to ensure that the heavy particulate matter that may have been in solution settles down to form a pellet at the bottom of the tube. The supernatant is then extracted and stored in a larger 5mL Eppendorf tube. The extracted sap solution is then further purified by passing it through Nalgene filter with a pore size of 0.2µm to completer the filtration process. The resulting solution should be a clear solution with a yellowish tinge. If the green tinge is still seen in the solution, the solution is again subjected to centrifugation for a longer time at 13,000 RPM until a pellet is formed at the bottom and the supernatant is extracted. The filtration process is repeated until a clear solution is obtained.

3.4.4 Soil Borne Wheat Mosaic Virus, Wheat Spindle Streak Mosaic Virus, High Plains Virus antibody and antigen

In this study the main focus is directed towards three major viruses that severely affect wheat, namely, wheat spindle streak mosaic virus (WSSMV), soil borne wheat mosaic virus (SBWMV), and high plains virus (HPV). WSSMV was first reported in north America in 1960 in Ontario, Canada, and then in Kansas in 1984. The three viruses in question are the antigens which are the target molecules, also obtained from Agdia inc., IN-USA.

The positive control for all the experiments, in this case the antigens, were prepared by reconstituting the vial in 500µl of phosphate buffered saline (PBS). The mixture was then mixed

uniformly by vortexing the vial at a rate of 3200 rotations per minute. The reconstituted material is now transferred to a 1.5mL sterile centrifuge tube. The centrifuge tubes are then subjected to centrifugation at the rate of 13,000 RPM for 2 minutes, until the supernatant is separated from the mixture. The supernatant is carefully extracted and is stored in 100µl aliquots at -20°C for short term storage and at -80°C in the long term. The aliquots are used as needed for experiments. All the three positive controls were performed in a similar manner and the obtained concentrations obtained for SBWMV, WSSMV and HPV are 17.7µg/mL, 26.8 µg/mL and 10.8 µg/mL respectively. The concentrations of the positive control aliquots are summarized in table 3.2 below.

Table 3.2: Summary of concentrations of prepared antigens

	Concentration
SBWMV	17.7ug/mL
WSSMV	26.8ug/mL
HPV	10.8ug/mL

Wheat spindle streak mosaic virus capture antibody (Agdia inc., IN-USA), soil borne wheat mosaic virus capture antibody (Agdia inc., IN-USA) and high plains virus capture antibody (Agdia inc., IN-USA) were all used in the immunoassay. In today's world, the antibody-antigen interaction property is one of the most commonly used techniques in affinity based bio-sensing or in general bio-sensing since antibodies bind to very specific protein molecules [46]. Antibodies are produced in the immune system on the introduction of the antigen or any foreign body into the system. In this case the plant viruses are injected into rabbits and the antibodies

that are produced to interact with antigens are then extracted. The production of specific antibody is a relatively straightforward process. The animal is immunized with the specific antigen. The immunization causes a response, with biosynthesis of antibodies against the injected molecule. Antigens must be prepared and delivered in a proper form and manner that maximizes the production of the specific immune response of the animal. The antibody generated is then purified by isolation of antibody from the serum, which can be done by three techniques- crude purification, general purification and specific purification. Crude form of purification involves the precipitation of a subset of the serum proteins that contain the antibody/immunoglobulin. General purification involves the purification to the extent of certain classes of antibody without regard to antigen specificity. Finally, specific purification involves the purification of those antibodies, that bind to a specific antigen molecule [47]. After purification, the antibody is then characterized by screening the antibody for specificity and affinity, measuring its concentration (titer) and determining its isotype, that is, its class and subclass.

Antibodies are generated to provide defense against foreign particles that enter the body. The structure of the antibody (or immunoglobulin) seen in the figure 3.15 are glycoprotein composed of one or more units, each containing four polypeptide chains: two identical heavy chains (H) and two identical light chains (L). The variable region refers to the amino terminal ends of the polypeptide chains, which shows a considerable variation in the amino acid composition. These differ from the constant regions which have a fixed composition of amino acids. Each light chain consists of one variable domain and one constant domain V_L and C_L respectively. The heavy chains consist of one variable region and three constant regions, with each heavy chain having twice the number of amino acids and molecular weight of a light chain. Heavy and light chains

are held together by a combination of non-covalent and covalent interchain disulfide bonds, forming a bilaterally symmetrical structure. The variable regions of the heavy and light chains serve as the sites for antigen antibody interaction- referred to as the antigen binding site. The hinge region is the area of the H chains between the first and second C region domains and is held together by disulfide bonds. This flexible hinge region allows the distance between the two antigen-binding sites to vary [48]. The arms of the heavy chains in the 'Y' structure have a variable F_{ab} section that are specific to the small class of target epitopes that are present on the target antigen. The primary amine of the heavy chain at the F_c region allows for the binding of the antibody to an NHS ester which allows the antibody to bind to the cross-linker molecule DSP, that is immobilized on the surface of the gold electrode in the immunoassay.

3.5 Immunoassay Protocol

There are two protocols followed during the construction of the immunoassay. The two separate protocols are used for two different experimental protocols. The first protocol is used to

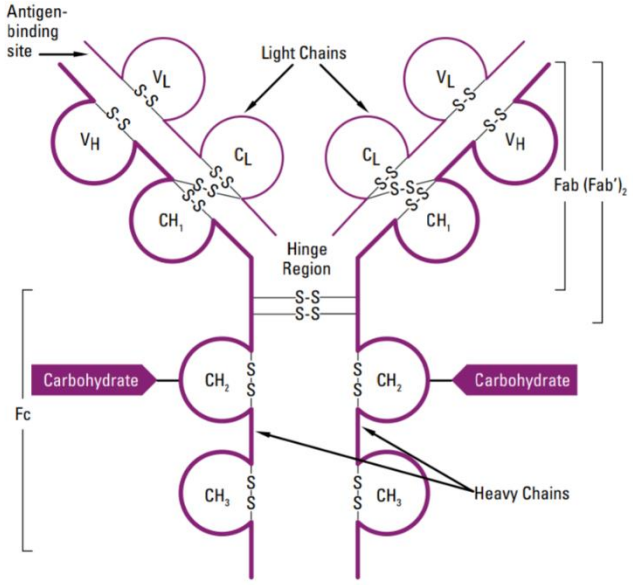

Figure 3.15: Structure of antibody/immunoglobulin

construct the immunoassay to independently characterize the antibody-antigen interaction in PBS buffer and to determine characteristics such as dynamic range, limit of detection and blank, which is the second specific aim of this work. The second protocol is used to construct the immunoassay to independently characterize the antibody-antigen interaction in complex plant sap buffer and to determine characteristics such as dynamic range, limit of detection and blank, which is the third specific aim of this work.

3.5.1 Protocol 1

The following protocol is used in the immunoassay construction for the independent characterization of the three viruses in a simple buffer- phosphate buffered saline. The electrochemical technique used in this whole experimental setup is electrochemical impedance spectroscopy (EIS). The sensors are prepared in the manner discussed in the sensor setup section, earlier in this chapter. With the sensors prepared, assembled appropriately, the whole protocol is followed for each individual chip. Each chip is to test multiple doses, in ascending order from the lowest dose to the highest dose.

Once the sensor is prepared, each individual sensor chip is functionalized with exactly 20µl of dimethyl sulfoxide (DMSO) (Thermo Fisher Scientific, Waltham, MA) is added to the sensing region. The DMSO is allowed to incubate for 5 minutes to remove any organic contaminants that may be present on the surface. The sensor is then dried with nitrogen an inert gas that does not react with the sensor surface. The sensor is then treated with an oxygen plasma for 30 seconds to remove any additional organic impurities that may be present on the sensor surface, additionally, it makes the surface extremely hydrophilic. DSP is added to the sensing region immediately after the plasma treatment and is allowed to incubate for 1 hour. This allows ample time for the DSP

to form a chemically cross-linked monolayer on the gold electrode. Additionally, the sensor is placed in a humidified chamber (to prevent the evaporation of DSP) in the dark, since DSP is light sensitive. After the DSP step is completed, the sensing region, should be aspirated well to ensure that it is dry, and care should be taken to avoid contact of any kind between the sensing surface and the pipette. Any contact or minute grazing may disturb the monolayer of DSP formed on the surface of the electrode. The next step would be to add 20 µl of PBS to the sensing region and allow it to sit for 30 seconds to remove any unbound DSP that may be present on the surface and to prepare the sensor for the addition of the antibody. The sensor should be aspirated and dried with nitrogen until no DSP or PBS remains on the surface. The antibody dose concentrations are stored in 20 µl aliquots at a concentration of 0.2mg/mL for HPV, and 0.4mg/mL for SBWMV and WSSMV. The antibody is serially diluted in PBS until a desired concentration of 10 µg/mL. 20 µl of the selected antibody is added to the sensing region and is allowed to incubate for a period of 1 hour. EIS measurements are taken after each wash step for a range between 1MHz to 1Hz.

The antigen dose concentrations are as summarized in table 3.2. The desired suspension buffer is PBS and a number of concentrations are required between 100fg/mL to 100ng/mL. The antigen is serially diluted and brought down in divisions of 10 to the desired lowest concentration. After the incubation of the antibody, doses of the antigen are added in regular intervals from the lowest dose of 100fg/mL to 100ng/mL in ascending order and is incubated for 20 minutes following which an EIS measurement for a range 1MHz to 1Hz is taken at each dose step. The procedure is repeated for the remaining two antibody and antigen pairs.

To account for the negative controls, the procedure remains the same until the addition of antibody. After the incubation of antibody, negative control experiments are performed in exactly the same manner as the positive control experiments, with increasing doses of the negative controls. For instance, let us consider an experiment is being performed with anti-SBWMV capture antibody immobilized on the gold electrode. Anti-SBWMV capture antibody is immobilized on 4 such sensor chips and each of the chips will have one experiment running on it simultaneously. The first chip will have the positive control, that is, increasing doses of SBWMV antigen. The second chip will have one negative control, either WSSMV or HPV and the third sensor chip will have the remaining negative control. Finally, the fourth sensor chip will have blank doses of PBS put on it to serve as the final negative control experiment.

3.5.2 Protocol 2

The following protocol is used in the immunoassay construction for the independent characterization of the three viruses in a complex buffer- plant sap. The electrochemical technique used in this whole experimental setup is electrochemical impedance spectroscopy (EIS). The sensors are prepared in the manner discussed in the sensor setup section, earlier in this chapter. With the sensors prepared, assembled appropriately, the whole protocol is followed for each individual chip. Each chip is to test a single dose, and not multiple doses as seen in the previous protocol. The reason for the change in protocol is done with the end application in mind. Since the biosensor is field based, it should be able to detect the presence of a random concentration of the virus in plant sap. The concentration of the virus in sap can vary according to the age of the plant and time it has been infected. Therefore, the protocol is changed slightly, with respect to the addition of the antigen in the final step.

The immunoassay protocol is the same with one additional step. Once the sensor is prepared, each individual sensor chip is functionalized with dimethyl sulfoxide (DMSO). The DMSO is allowed to incubate for 5 minutes to remove any organic contaminants that may be present on the surface. The sensor is then dried with a stream of nitrogen gas. The sensor is then treated with an oxygen plasma for 30 seconds to remove any additional organic impurities that may be present on the sensor surface. DSP is added to the sensing region immediately after the plasma treatment and is allowed to incubate for 3 hours. After the DSP step is completed, the sensing region, should be aspirated well and at the next step 20 µl of PBS is added to the sensing region and is allowed to sit for 30 seconds to remove any unbound DSP that may be present on the surface and to prepare the sensor for the addition of the antibody. The sensor should be aspirated and dried with nitrogen until no DSP or PBS remains on the surface. 20 µl of 10 µg/mL of the antibody is added to the sensing region and is allowed to incubate for a period of 4 hours in a humidifying chamber. EIS measurements are taken after each wash step for a range between 1MHz to 1Hz. After this step, a blocking protein, super block is added to the immunoassay. Superblock is a large protein molecule that bind to the free unbound ends of the DSP and thereby minimizes any non-specific interaction of the antigen with the DSP. Non-specific interactions of the antigen produce an undesired response and an increase in the noise of the system, which then impacts signal to noise ratio of the system.

The antigen dose concentrations are as summarized in table 3.2 in an earlier section. The desired suspension buffer is plant sap and a number of concentrations are required between 100fg/mL to 100ng/mL. The antigen is serially diluted in plant sap and is brought down in divisions of 10 to the desired lowest concentration. After the incubation of the antibody, doses of the antigen are

added to each chip from the lowest dose of 100fg/mL to 100ng/mL and an EIS measurement for a range 1MHz to 1Hz is taken at each step.

In order to establish that the sensor is able to distinguish one virus from another, a cross reactivity study is performed. For this study, sensor parameters such as specificity, and sensitivity are studied. The reaction of an antigen to its own antibody and the reaction of other antigens with the chosen antibody is studied. The protocol is appropriately changed to have one single dose on one chip, for discreet measurements, and therefore, for resource management purposes, the number of chips per experimental set are reduced to 5, with three doses accounting for the specific antigen molecules (positive control) and two doses accounting for the negative control (non-specific antigen molecules) experiments. If the entire dose range is to be done for each chip, then there would be a requirement of 7 chips per experiment set, and with one positive control and 3 negative control sets which is wasteful and unnecessary. To account for non-specific interactions, a single negative control bio-molecule is chosen based on ELISA results performed elsewhere, among the remaining two viruses and is added to the prepared immunoassay. Therefore the 5 sensor chips would have 3 concentrations of the positive control added independently on each of the 3 sensor chips and the remaining two will have two doses of the negative control added independently on the remaining two sensor chips.

CHAPTER 4

RESULTS AND DISCUSSION

4.1 Baseline Measurements

A number of factors such as total surface area of the sensing electrode, output impedance, signal to noise ratio, sensitivity among other sensor parameters, influenced the choice of electrode chosen to undertake the work presented in this thesis. While the sensor parameters and the theoretical soundness of the design are important, it is crucial to establish the baseline response for all the electrode designs. EIS measurements are performed for all baseline experiments, for n=3 sensor chips with 5 wash steps of standard 1mM PBS added to the sensing area. The summary of the experimental parameters used for EIS are summarized in table 4.1 below.

Table 4.1: Summary of experimental conditions for EIS

Technique	EIS
Initial Frequency (Hz)	1000000
Final Frequency (Hz)	1
Points/decade	10
AC voltage (mV RMS)	10
DC Voltage	0
Area (cm^2)	0.5

Other baseline tests include determining the stability of the electrodes over a time period, for which a couple of other experiments are designed. The open circuit potential and the single

frequency EIS experiments are carried out for a time period of 1 hour and 20 minutes respectively and the data is observed to measure its stability.

4.1.1 Baseline- Design version 1

After the sensor fabrication process and the senor preparation step, both discussed in earlier sections of this thesis, the electrode design is now ready for its baseline experiments. The multiplexed sensor design has three working electrodes and one reference electrode as shown in figure 3.1. Wires are adhered to the electrode using epoxy, which is a two-part mixture, when mixed in equal parts and heat cured for ten minutes, forms a conducting bond between the sensor's conducting pads and the wire. The electrodes are interfaced with the Gamry potentiostat 600. 150µl of PBS buffer is added to the sensing region and EIS is performed on the sensor. The experimental conditions are summarized in the table 4.1.

By measuring the impedance response to the applied AC signal, the consistency of the impedance response obtained for multiple washes of the same buffer (1mM PBS), is obtained and recorded. All factors for the experiment are kept constant.

Figure 4.1 shows the impedance response for electrode design 1 shown in figure 3.1. The baseline was conducted for n=3 chips and the average data from the sensor chips are depicted in figure 4.1. The response is extracted for a frequency of 100Hz since there is maximum double layer capacitance at that particular frequency range. The response for each wash step from electrode 1 to electrode 3 is visibly distinguishable from each other. There is a maximum variability of 30.53% across electrodes, measured by the maximum difference of the mean baselines of electrodes 1,2 and 3. The mean baseline readings of electrode 1 and electrode 3 appear to have a similar range of 2KΩ to 2.5 KΩ. The data shows that 2 out of 3 electrodes have

similar baselines, however, if we consider the error bars and the standard deviation across n=3 chips, large error bars which indicates that there is a large variation of baselines from chip to chip. The chip to chip variability was found to be 37% which can be attributed to the non-uniform coverage of the sample on the surface of the electrode or due to cross talk between the electrodes. The two variabilities combined, make electrode design 1 very inconsistent. Another

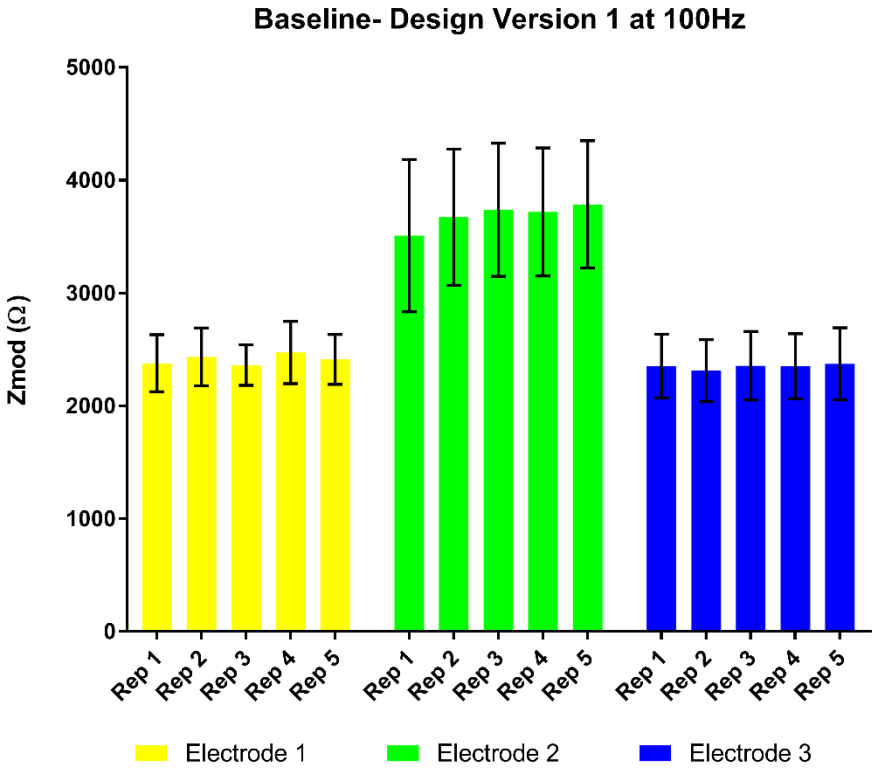

Figure 4.1: Baseline - Design Version 1

possible factor that could have attributed to the variability is the electrode orientation. Although they are of the same dimension, electrode 1 and electrode 3 are aligned vertically with respect to the reference electrode, whereas, electrode two is aligned horizontally. Although the design is sleek, there are practical issues with the electrode. Multiple methods were tried to try and confine the liquids to their respective electrodes, however, because of the limited spacing between the

electrodes and the high hydrophilicity of the solutions used in the immunoassays, it was impossible to contain the fluid onto its designated electrode.

4.1.2 Baseline- Design version 2

Electrode design version 2 was designed because of the practical shortcomings of design 1. The multiplexed design, similar in arrangement to version 1, varies only by the shape(circular) of the working and reference electrodes as shown in figure 3.5. The change in shape allows for the increased spacing between the working and reference electrodes. The spacing between the sensors is increased to 1.75mm as opposed to 0.75mm in the flagship multiplexed design. The sensors are setup as described earlier in this thesis and are interfaced with the Gamry 600 potentiostat. EIS is carried out with the exact same parameters shown in the table 4.1. the only difference between the conditions for EIS is that the surface area parameter in increased to 1.5cm^2. The experiment is carried out for n=3 sensor chip, and the average data from the three are plotted and shown in the figure 4.2.

The data is extracted at 100 Hz since the bode phase plot shows a maximum capacitance at that particular frequency range. From the data obtained, the impedance response between washes has a maximum variability of 27% between the lowest and highest recorded mean values, across all three electrodes. The error bars on indicate the large chip to chip variability, recorded at 26% which is undesirable. The impedance values are on the lower side in comparison to electrode design 1 at 100 Hz which is attributed to the increase in the size of the electrodes. Consequently, small changes in dose response may go unnoticed with this electrode design. Overall, the design showed less variability than version 1 with the only positives being that the selective immobilization was achieved without the use of any encapsulants or physical

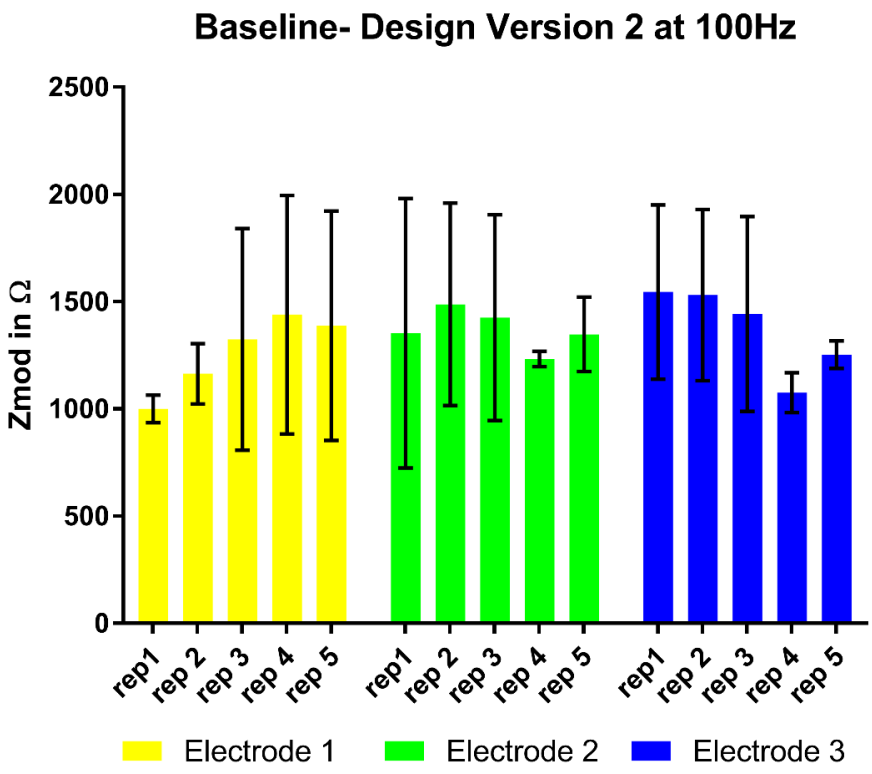

Figure 4.2: Baseline - Design Version 2

separators. The reasons for the high variability seen with this electrode could again be attributed to the cross talk between electrodes as well as the improper distribution of the fluid on the sensing area.

4.1.3 Baseline- design version 3

While the first two designs presented us with significant advantages of immobilizing three separate biological fluids on the same electrode which in turn would make it capable of detecting three different target molecules. However, the unstable baselines, chip-to-chip variability and practical difficulty to immobilize fluid on the electrodes make these two designs unsuitable moving forward. With the third design, we move away from using multiple working electrodes

on a single chip because of the variability in baseline between electrodes on the same chip and the difficulty in immobilizing three different biomolecules on the same sensor chip which is evident in the design versions 1 and 2. With Design version 3, we move away from gold on glass and introduce the electrodes manufactured on a printed circuit board. Design version 3 is chosen and is a well-established sensor design used in many affinity based bio-sensing applications [34] [49] [50].

The sensor comprises of a two-electrode system, with all electrodes having a trace width of 1mm and with 1mm gaps between each edge. The working and reference electrodes were patterned on the PCB in an interdigitated concentric circular design as shown in figure 3.8.

The sensor chip is prepared and interfaced with a Gamry 600 potentiostat. EIS is carried out with the conditions shown in table 4.1, changing only the surface area parameter, which is at 1.5cm^2. The experiment is carried out for n=3 sensor chips, and the average data from the three sensors are plotted and shown in the figure 4.3.

The bode phase plot, reveals that the region of maximum double layer capacitance is in the region of 100 Hz and therefore, all data is extracted a 100Hz frequency. From the data obtained, it is seen that impedance washes between sensor chips is minimal and very stable and only has a variation of 13% between washes. The tight error bars indicate that there is minimal variation from chip to chip (8%). Overall from the baselines, it is evident that the sensor is robust and stable, however, the only disadvantage with this sensor design was its size and consequently, the impedance values were very low at the selected frequency. Moreover, the increase in the size of the sensor, meant that a larger volume of buffer was required, which was undesirable, not

because of the lack of resources, but because, the same objective can be achieved, with the same accuracy, with smaller volumes, which is addressed in design version 4.

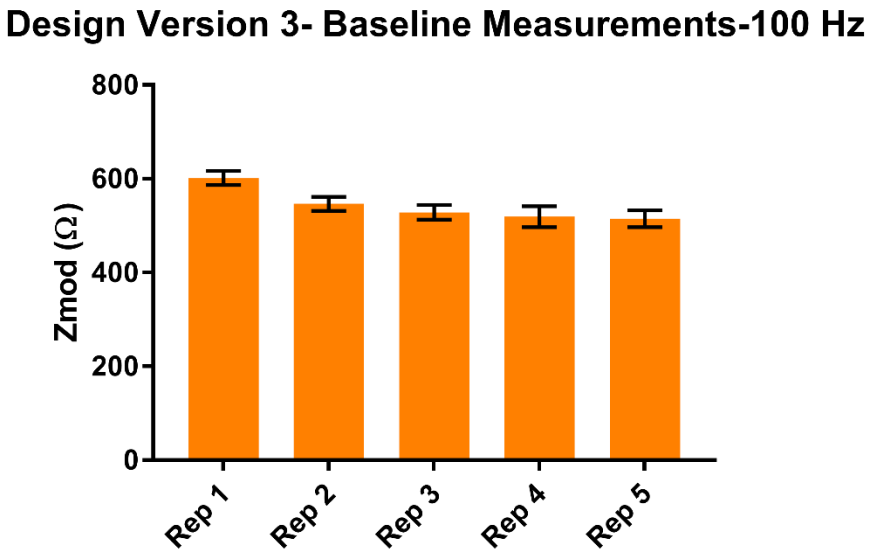

Figure 4.3: Baseline -Design Version 3

4.1.4 Baseline- Design version 4

The disadvantages presented by design version 3, provided the pathway for the 4th and final electrode design. The electrode design again is a two-electrode system, with a hook like reference electrode, enveloping the working electrode. The electrode is much smaller in size compared to version 3 and is patterned on a PCB substrate as shown in figure 3.11.

The sensor is setup and is interfaced with a Gamry potentiostat 600. EIS is performed for n=3 sensor chips with the EIS parameters shown in table 4.1. There are multiples changes that accompany this design. The total surface area of the sensor is reduced massively to a tiny area of 0.01cm^2, which meant that 20µL of PBS buffer was a sufficient volume to cover the sensing region of the sensor. The overall design is changed to a simpler hook shaped electrode as

opposed to the interdigitated concentric rings of gold that is seen in the previous design. The baselines were measured with standard EIS performed for a range between 1 Hz and 1MHz.

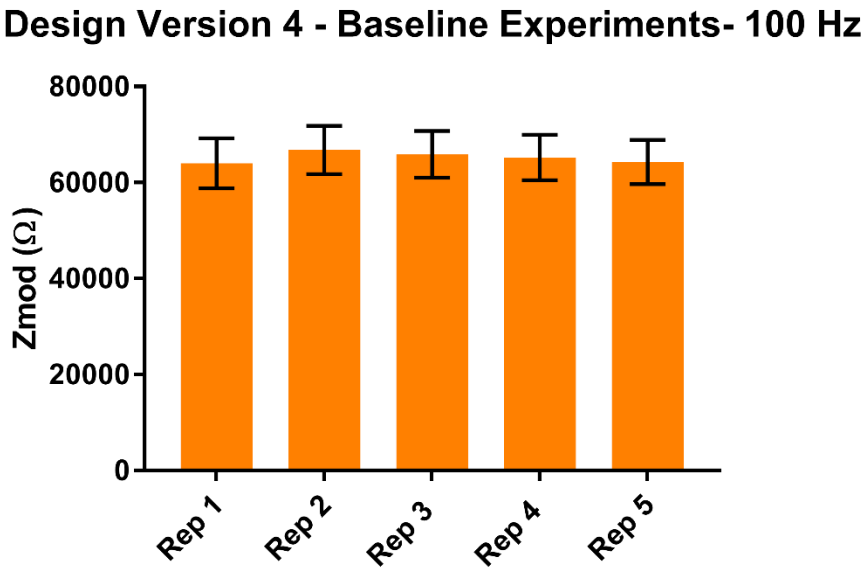

Figure 4.4: Baseline- Design version 4

The impedance response once again extracted at 100Hz, shows a much higher baseline impedance than the previous sensors, in the range of 65-80KΩ as opposed to the 500-700Ω range observed for the same volumes. The high values of impedance seen for the baselines in figure 4.4 means that smaller changes in concentration can be detected and doses at lower concentrations can be distinguished from each other. The chip to chip variability is close to 15%, indicated by the error bars on each wash step. Now although the chip to chip variability is leaning towards the higher side, it is not a cause for concern since we normalize all readings with respect to the baselines for all the measurements made during an experiment. Across the five wash steps, a minimal variation in the baseline is observed. The high impedance values, the low variability

between wash steps, the low volume makes electrode design version 4 a favorable choice for the multiplexed detection of plant pathogen.

4.1.5 Single Frequency EIS and Open Circuit Potential Experiments

Apart from the short circuit EIS experiments and the COMSOL models to establish the feasibility of the electrodes, there were two other experiments carried out as additional baseline experiments to show the stability of the electrodes. A single frequency EIS measurement was performed for 20 minutes and an open circuit (OCP) measurement was performed for 1 hour on each electrode system with a sample period of 0.5 seconds. The two aforementioned experiments provide information of the electrode stability over time. Whenever the potential of an electrode is forced away from its value at open-circuit, that is referred to as “polarizing” the electrode. When an electrode is polarized, it can cause current to flow through electrochemical cell and consequently reactions that occur at the electrode surface.

In cells where an electrode undergoes uniform corrosion at open circuit, the open circuit potential is controlled by the equilibrium between two different electrochemical reactions. One of the reactions generates cathodic current and the other generates anodic current. The open circuit potential equilibrates at the potential where the cathodic and anodic currents are equal. It is referred to as a mixed potential. If the electrode is actively corroding, the value of the current for either of the reactions is known as the corrosion current. Open circuit potential, for this reason is also referred to as corrosion potential. For a stable electrode system, the open circuit potential should not vary with time, and should remain at a constant voltage, as close to 0 as possible.

Single frequency EIS is a technique wherein, the impedance response of a sensor is measured at a particular frequency. Essentially, it is the same as EIS, with the only difference being, EIS measures the impedance response of the sensor over a range of frequencies. Single frequency EIS is used in impedance-based sensor development to monitor changes in the impedance values over time. Again, it is desirable to have minimum drift or variation in impedance values over time. The table 4.2 summarizes the experimental conditions used for single frequency EIS.

Table 4.2: Summary of experimental conditions for single frequency EIS

Technique	Single Frequency EIS
Frequency (Hz)	100
AC voltage (mV RMS)	10
DC Voltage	0
Area (cm^2)	0.5
Total time (minutes)	20
Repeat Time(minute)	0.01

From the data obtained (shown in figure 4.5), it is observed that the single frequency measurements for version v1 (part i.-figure 4.5) has the maximum drift and its value changes by 45% over 20 minutes. Version 2 (part ii) meanwhile has a flatter line, with variation of 4.5% and does not vary so much with time. Version 3 (part iii) shows the least variation over time at a change of 0.1% and is the most stable among the 4 designs. Finally design version 4 (part iv) is seen to have a variation of 0.3% over 20 minutes and its stability is comparable to that of design version 3 and therefore is very stable. The single frequency data is plotted in figure 4.5.

To summarize, four main aspects are looked at with respect to baseline measurements. First, COMSOL modelling is performed to establish the theoretical feasibility of electrode design. Strong electric fields and current densities are observed in the designs, which facilitates easy charge transfer.

Secondly, impedance response from EIS studies are looked at, which from data, shows us a very low variability from sensor to sensor after multiple washes for design versions 3 and 4.

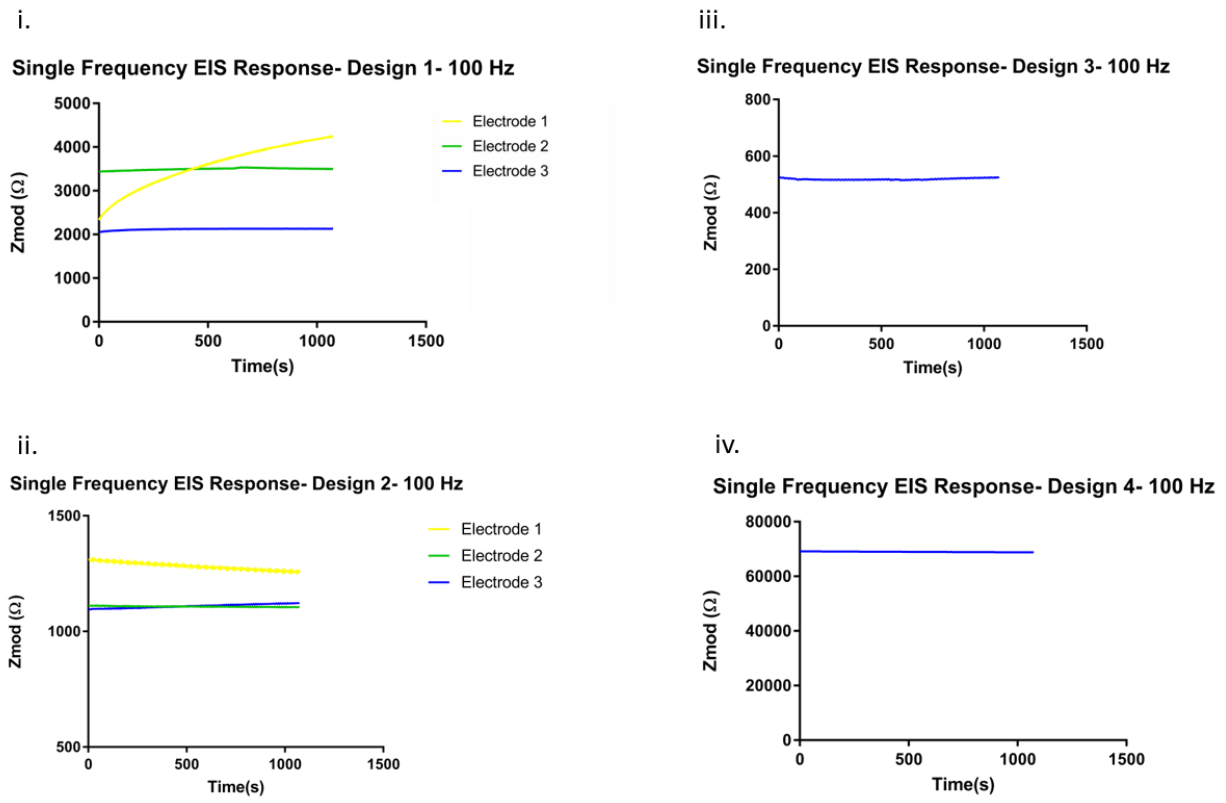

Figure 4.5: Single frequency data for all electrode designs at 100 Hz for 20 minutes

Third, single frequency data is evaluated, which show us that the impedance values for the 3rd and 4th design have least variation over time. Finally, OCP values for the third and 4th designs are evaluated since they both have comparable stabilities based on previous tests. The first two

electrode designs have been deemed unstable because of the unstable design and baseline parameters. The OCP of design version 3 and 4 are shown in figure 4.6 where the x-axis represents the time in seconds and the y-axis depicts the open circuit potential in volt.

It is observed that the two OCPs over time are extremely stable and very close to 0, which is a desirable characteristic. The two designs are very comparable and the only factor that tips the selection of design version 4 is a parameter known as signal to noise ratio (SNR). Signal to noise ratio is defined as is defined as the comparison of the strength of a desired signal to the level of background noise produced by the system. It is always desirable to have a high SNR for any system since it gives us the level by which a system is able to differentiate useful and meaningful information from the noise.

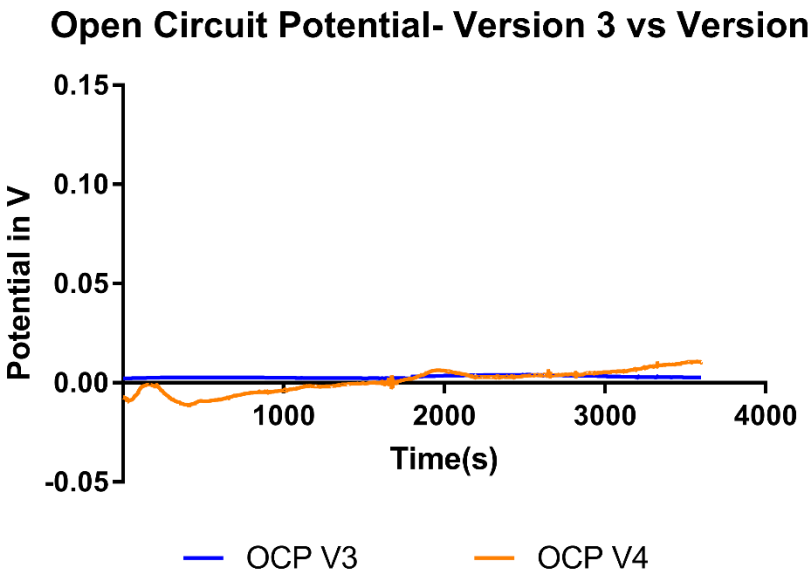

Figure 4.6: Comparison of open circuit potential version 3 vs version 4

The SNR of the systems can be determined by performing a full immunoassay experiment, with the desired protocol and then measuring the SNR of each of the systems based on the data output from the experiments. The full experimental protocol is followed as depicted in section 3.5.1.

After performing the experiments and extracting the required data, three data points are chosen corresponding to a low dose (10 pg/mL), a medium dose (1 ng/mL), and high dose (100 ng/mL). A standard EIS experiment was performed for each step for a frequency range between 1Hz-1MHz for n=3 replicates. The results are plotted in parts i. and ii. (figure 4.7) which denote the response from design versions 3 and 4 respectively, and the data is compared. The x-axis depicts the three doses and the y-axis depicts the normalized impedance with respect to the baseline at the antibody step, that is, the value of impedance at each dose step divided by the maximum baseline impedance value at the antibody step. The SNR is determined by calculating the magnitude of maximum signal obtained divided by the maximum value of limit of blank (denoted by the dashed black lines in the figure 4.7) It is found that the maximum SNR for design version 3 is 1.6 whereas design version 4 was found to have a maximum SNR of 3.

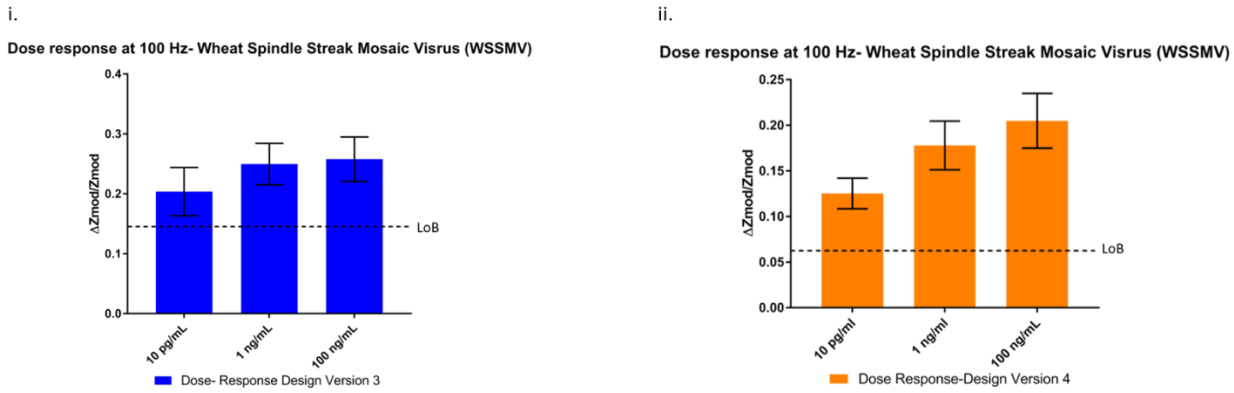

Figure 4.7: Comparison of SNR for Design version 3 vs version 4

Having looked at these aspects the electrode design 4 configuration is chosen as the sensor chip which is most stable and appropriate, moving forward. With the baseline stability established, any changes or perturbations in the signal can be attributed the functionalization and interaction at various points in the immunoassay and not the setup of the sensor.

4.2 Immunoassay

There are two immunoassays built during the course of the entire work. With the first immunoassay to establish the proof of concept of the whole working in simple buffer solution and the second to establish sensing the target biomolecule in plant sap. The steps for building the immunoassay has already been discussed in chapter 3. The main focus of this section would be to establish that the antibody binds to the cross-linker molecule and to establish that various doses of the antigen subsequently binds to the antibody.

4.2.1 Antibody binding

The protocol for the functionalization of the antibody is discussed in chapter 3 and follows exactly the same protocol. To ensure that the antibody is bound to the surface EIS is performed to monitor changes in impedance of the sensor after subsequent assay steps. Changes in impedance will correspond to binding that is occurring between the antibody and crosslinker. Zmod was evaluated for this study. Zmod is the sum of both real and imaginary parts of the impedance response, which indicates the resistive and capacitive changes in the electrical double layer. All steps use a sample volume of 20µL, that is added to the sensing region.

First, PBS is added to the sensing region on a freshly prepared sensor surface to create a baseline comparison for the other immunoassay steps to follow. A full range EIS measurement is recorded. The sensor is then dried, plasma treated and immediately after DSP in DMSO is added to the sensing surface and is allowed to incubate. Another EIS measurement is made at this step. Soon after the incubation of DSP, a PBS wash was conducted to wash away or remove any unbound DSP lingering at the surface. An EIS measurement is now made, with changes in

impedance from the DSP step compared to the PBS wash step sheds light on the binding of DSP to the electrode surface. The sensor is then incubated with antibody after which, another EIS measurement is taken. The sensor is now subject to five PBS washes and the impedance values are recorded at each step. If there is minimal change between the antibody step and the impedance reading at the fifth wash step, it validates that the antibody is indeed bound to the surface. Table 4.3 summarizes the experimental conditions used for the antibody binding study.

Table 4.3: Experimental conditions for antibody binding study

Technique	EIS
Frequency (Hz)	100
Sample volume	20 µL
Antibody concentration	10 µg/mL (anti-SBWMV capture antibody)
Replicates	3

As indicated earlier, the PBS short circuit measurement will be chosen as the reference point or point of comparison for all other steps to follow. The data in figure 4.8 reveals that the average baseline impedance is at 130KΩ. The large increase in impedance seen after the DSP incubation is attributed to the resistive nature of the DSP in DMSO solution. The subsequent step- PBS wash after the incubation of DSP and the average decrease in impedance of 20KΩ compared to the baseline/short circuit value of PBS indicates that DSP is bound to the surface. After the incubation of the antibody, it is seen that the impedance values drop further as a result of charge conduction nature of the antibody. The average value of impedance drops to 69.8 KΩ. The difference in all these functionalization steps are observed to be significantly different from each

other. To ensure that the antibody remains bound to the surface, subsequent washes of PBS was conducted (indicated by the zerodose step in figure 4.8) after the antibody step and measurements were recorded at each step. It is seen that the average value of impedance almost remains the same with the average impedance rising only by 500Ω. It is evident that there is no observable change between the subsequent wash steps, with minimal change in the impedance values from the antibody. Therefore, it can safely be established that the antibody is successfully bound to the surface of the electrode.

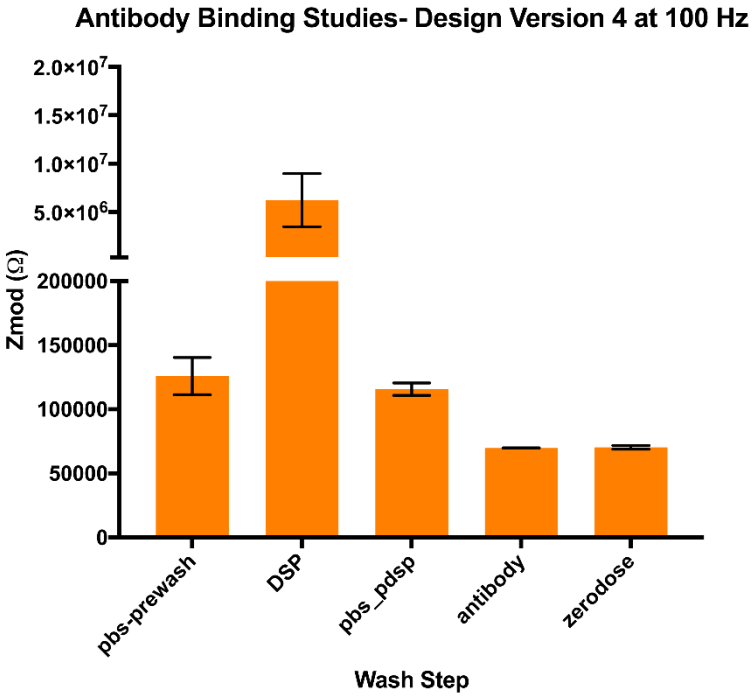

Figure 4.8: Antibody binding studies at 100Hz

4.2.2 Antigen Binding in simple buffer-Phosphate Buffered Saline (PBS)

After confirming that the antibody is bound to the surface of the electrode, the next step in the immunoassay process is to check the binding of the antigen molecule. The focus of specific aim

2, which is to ensure that there is binding of antigen in a simple PBS buffer. The three antigens involved are, soil borne wheat mosaic virus (SBWMV), high plains virus (HPV), and wheat spindle streak mosaic virus (WSSMV).

All antigens are prepared in the process described in chapter 3 and serially diluted to the desired concentrations. A dynamic range of 100fg/mL to 10ng/mL is tested and analyzed. EIS is used to validate the level of antigen bound to the antibody. Four sensors are prepared and individually functionalized with antibody. The first sensor is used for the positive control, with the other three being negative controls. The negative controls involve the addition of the other two non-specific molecules to the antibody immobilized on the surface for sensor 2 and sensor 3. Finally, sensor 4 is treated with multiple washes of blank PBS, commonly referred to as zero-dose response. The impedance change across the dose steps was evaluated to see if there was a change in impedance. Table 4.4 summarizes the experimental conditions used for the EIS experiments.

Table 4.4: Summary of experimental conditions for antigen binding studies

Technique	EIS
Frequency (Hz)	9
Sample volume	20µL
Buffer	10mM PBS
Antigen concentrations	100fg/mL, 1pg/mL, 10pg/mL, 100pg/mL, 1ng/mL, 10 ng/mL, 100 ng/mL
Replicates	3

First, soil borne wheat mosaic virus (SBWMV) is analyzed over the given dynamic range, shown in figure 4.9. At each dose step, there is a noticeable decrease in the change in impedance with respect to the antibody functionalization step. These results actually correspond to the actual decrease in absolute impedance with increase in doses, which implies that the immunoassay becomes more conductive and therefore there is binding occurring at the surface of the electrode. For ease of analysis, the change in impedance of the dose is calculated from the previous step, and the ratio of the change of impedance value Mod[z]/Zmod is to the baseline impedance value Mod[z] at the antibody functionalization step is plotted for every value. This step allows the normalization of data across chips and makes it easier to plot for n=3 replicates, and the normalization multiplied by a factor of 100 gives the % change across each step with respect to baseline. All values extracted from the data are in terms of this ratio. On evaluating the dose response, it is concluded that the average maximum change for the highest dose is close to 25% with a noticeable change in impedance response for each step with respect to the baseline. The dose response is plotted against the negative control experiment with blank PBS washed to determine the extent of dose dependent response to zero-dose response. The zero-dose response, plotted in the form of a dashed-line, shows a maximum average variation of 12% at the 6^{th} blank PBS wash. On comparing the maximum signal output to the maximum value of baseline for zero-dose response, the signal to noise ratio is calculated and is found to be 2. Furthermore, the limit of detection, defined as the sensor's capability to accurately measure and distinguish the smallest analyte concentration from the analytical noise signal. The signal produced in the absence of analyte is called "analytical noise", in this case the zero-dose response [51]. On evaluation of the data after extrapolating the maximum noise signal, it can be seen that the limit

of detection for the SBWMV assay is at 10 pg/mL. LoB is estimated by measuring replicates of a blank sample

and calculating the mean result and the standard deviation (SD) [52].

LoB = mean blank + 1.645(SD blank)

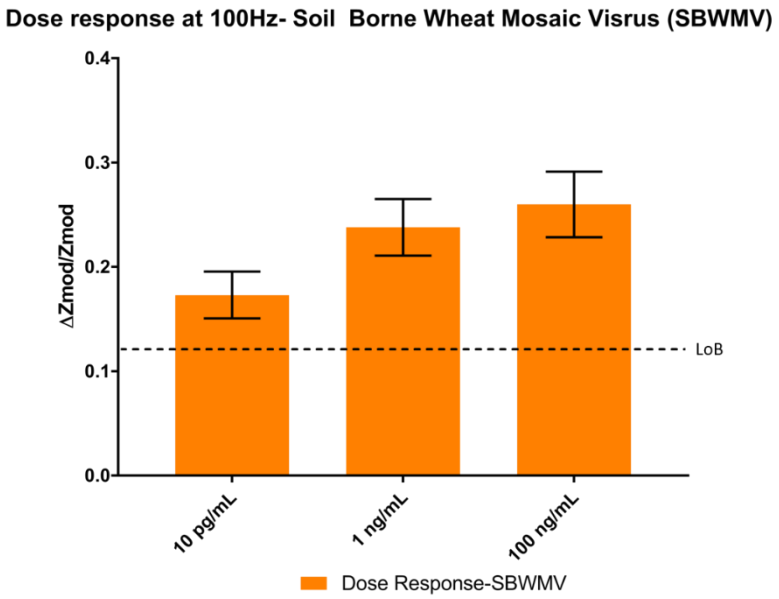

Figure 4.9: Dose response of soil borne wheat mosaic virus at 100Hz

Second, wheat spindle streak mosaic virus is studied, and the same parameters are evaluated. From the figure 4.10, it is again evident that a dose dependent change is seen, reflected by the change in the ratio of the impedance change to the baseline at the antibody step. The LoD again is seen to be 10pg/mL concentration of the WSSMV and the maximum SNR from the data is 2.8 with a LoB at 0.7. Figure 4.8 shows the dose response of the WSSMV antigen on the immunoassay built with the anti-WSSMV capture antibody. The large error bars could indicate that the bio-molecule is highly active, or it could simply indicate the chip to chip variability.

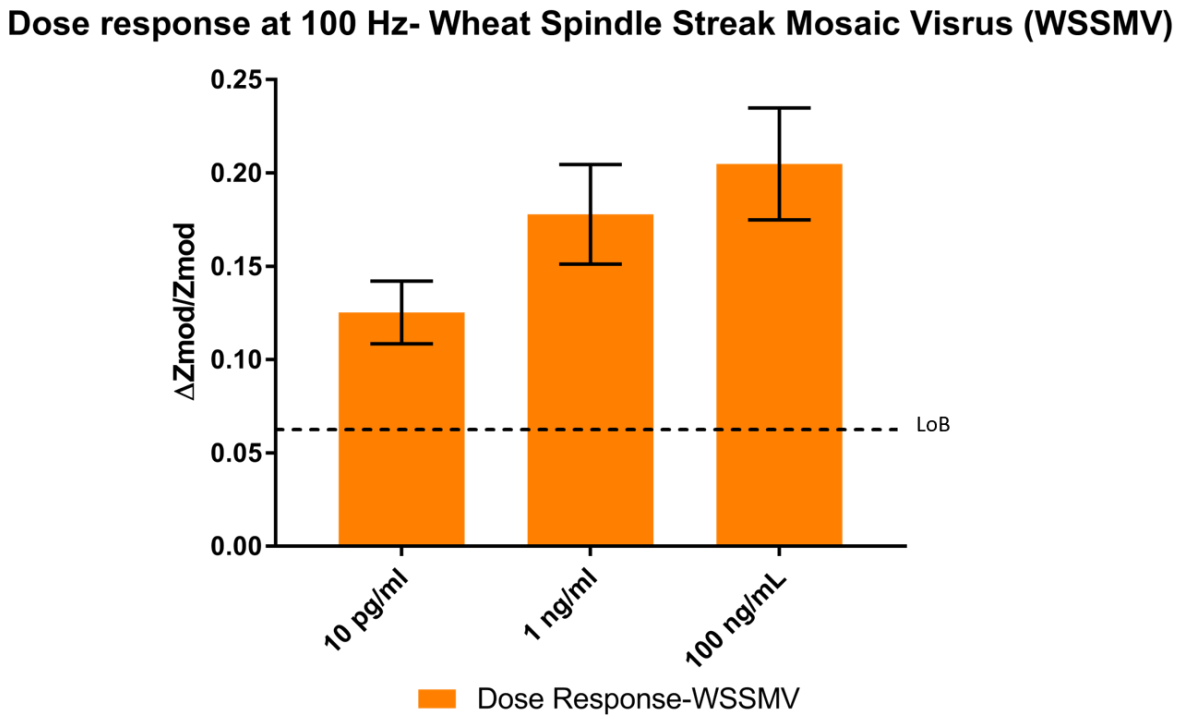

Figure 4.10: Dose response of wheat spindle streak mosaic virus at 100 Hz

Lastly, high plains virus is the final bio-molecule evaluated and the dose response is shown in figure 4.11. On evaluation of the data, it is similar to the two previous molecules, that is, SBMWV and WSSMV in terms of response. The LoD from the data is again, 10pg/mL which is the same as the first two molecules. The SNR is calculated to be around 2.2 and finally, the limit of blank is found to be 0.09. The dynamic range for all three bio-molecules are from 10pg/mL to 100ng/mL. The table 4.5 summarizes the parameters determined from the data above for the characterization of plant pathogen in simple buffers. While the protocol establishes the proof of concept of the affinity based biosensor, there is a definite issue which has to be addressed. The two other negative controls showed a positive response for a non-specific antibody. The impedance response, was less than the magnitude of response is attributed to the exposed surface

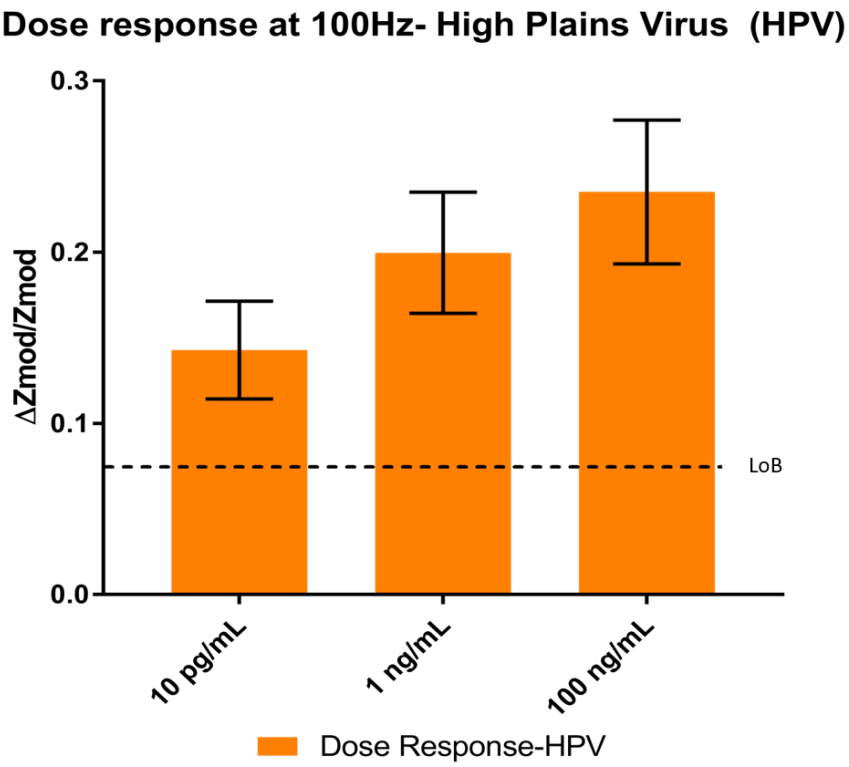

Figure 4.11: Dose response of high plains virus at 100Hz

Table 4.5: Summary of data from antigen binding experiments

	DYNAMIC RANGE	Limit of Detection	SNR	Limit of Blank
SBWMV	100 fg/mL-100ng/mL	10 pg/mL	3	0.12
WSSMV	100 fg/mL-100ng/mL	10 pg/mL	2.8	0.07
HPV	100 fg/mL-100ng/mL	10 pg/mL	2.2	0.09

area on the electrode surface between the antibody. This surface is bare and small molecules can interact with these surfaces causing a response and a non-specific signal response. The non-specific response however, does not interfere with the results showing the dose dependent changes that were discussed earlier. In order to overcome this, an extra step is added to the immunoassay, which helps overcome this problem.

4.2.3 Antigen binding in complex buffer-Plant Sap

The third aim to characterize the three viruses of interest in a complex buffer media, namely plant sap. The preparation of sap is discussed in chapter 3 of this thesis. The prepared sap is to be treated as a regular buffer and any antigen preparation would be prepared in the exact same way as one would with PBS.

Due to the optimization of resources, the design of the experiment is slightly changed with the objective being the same. After having established the proof of concept in specific aim 2, specific aim 3 looks to repeat the same set of experiments, with the only difference being the buffer media in which the antigen is suspended. The design for this experiment includes 3 specific doses and a common non-specific molecule with 2 doses. A Common non-specific molecule is chosen based on ELISA tests conducted elsewhere, where HPV was shown to be the most stable non-specific molecule. The three positive control doses include a low dose, medium dose and a high dose while the non-specific negative control contains a high dose and a low dose. The design is changed from the standard dose dependent response since the end application for this senor will be a field based device whose objective would be to deal with a range of concentrations. The sensor chip should be able to show binding in either case, be it a dose dependent change, or a discrete change for a specific concentration.

The construction of the immunoassay is already discussed in section 3.5.2 of the thesis. The only difference being the addition of SuperBlock^{TM} to the immunoassay helps overcome the non-specificity issue faced in specific aim 2. SuperBlock is a blocking buffer whose main constituent is PBS along with a blocking protein that effectively blocks exposed areas of electrode surface that react with a non-specific molecule and introduce noise into the system. The protein based formulation does not contain any immunoglobulins or antibodies making it compatible in situations where traditional blocking agents fail.

The protocol is the exact same up until the binding of antibodies on the surface of the electrode. After this step superblock is introduced and is allowed to incubate for 20 minutes, after which a standard EIS scan is conducted. The surface is now dried and washed with PBS to wash away any excessive unbound proteins. Another standard EIS measurement is conducted with the summary of all experimental conditions summarized in table 4.6.

Table 4.6: Summary of conditions for antigen binding experiments in complex buffer

Technique	EIS
Frequency (Hz)	100,300,500
Sample volume	20µL
Buffer	Plant sap
Antigen concentrations	1pg/mL, 10pg/mL, 100pg/mL, 10 ng/mL
Replicates	1
Negative Control	HPV/SBWMV

After the PBS wash step, the antigen is added in discrete concentrations mentioned in the table above. The three concentrations for the specific doses were 1pg/mL, 100pg/mL, and 10 ng/mL while the concentrations of the non-specific, negative controls were 10 pg/mL and 10 ng/mL. The chosen antigen is allowed to incubate for 30 minutes before a measurement after which an EIS measurement was taken with the conditions shown in the table 4.6.

The data in figure 4.12 shows the response of the sensor to the addition of both specific and non-specific molecules. All changes in impedance of the dose is calculated with respect to the antibody functionalization step, and the ratio of the change of impedance value Mod[z] is to the baseline impedance value Mod[z] at the antibody functionalization step is evaluated for every step. The ratio then multiplied by 100 gives the % change in signal with respect to baseline. The y-axis represents this percentage change while the x-axis represents the dose steps.

Discreet doses of SBWMV suspended in sap was added to the electrodes individually and the impedance response for SBWMV was extracted at 100 Hz. 100 Hz was chosen from the bode phase plot, which was the region at which maximum capacitive change at the electrical double layer was observed. The impedance response is recorded at this frequency for all doses. The dose response shows a positive trend in the impedance change of the signal. The positive percentage change indicates that the impedance is decreasing with respect to the baseline. Once again, mod[z] measurements are evaluated, which is a sum of both real and imaginary parts of the impedance. The decreasing impedance would mean that the surface becomes more conducting. The positive trend in the impedance, is completely opposite to the change exhibited by the non-specific molecule or the negative controls. The negative control exhibits a trend that is opposite,

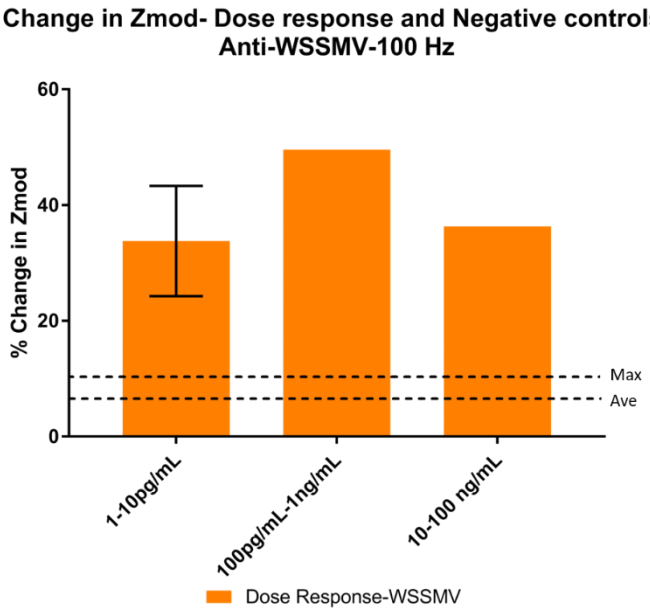

Figure 4.12: Dose response of wheat spindle streak mosaic virus (WSSMV) at 100 Hz

that is, the impedance seems to increase or remain close to the baseline impedance, on addition to the immunoassay which could indicate that there is no binding occurring. The negative control used for the experiment is HPV which also helps us tackle the cross reactivity. The negative change in percentage, is indicative of the increase in zmod, which means that solution is becoming more resistive, which can be attributed to surface adsorption. Additionally, the increasing trend of zimag is observed for the dose response and the decreasing trend for the negative control (data not shown) which sheds light on the manner of binding taking place at the electrical double layer. The dose response shows a maximum change of 46% while the negative control shows a maximum of -12%. To make interpretation easier, the modulus of the delta change with respect to the baseline is taken and plotted. The inference from the figure 4.11, shows that the maximum dose response at 46% is much higher than the maximum noise generated due to the non-specific interaction with the antibody, with a maximum SNR of

approximately 4. The trends of the dose response and negative control clearly distinguish themselves from each other, and therefore, it can be established that the doses of SBWMV is detected successfully.

The figure 4.13 shows the unmodified and unedited trends that are obtained before processing the data. HPV is used for the negative control experiment. The experimental conditions and the recording of data is done in the same manner described earlier in this section. From the figure 4.13 it can be seen that the negative controls follow a negative trend, hovers around the zero line or is very close to zero for both doses. The maximum dose response for the positive control is recorded at 45% while the maximum value for negative control is at -12%. Since there is no noticeable change from the baseline for the negative control, it is concluded that no binding is occurring. The large error bars indicate a larger variation in signal response. The columns with

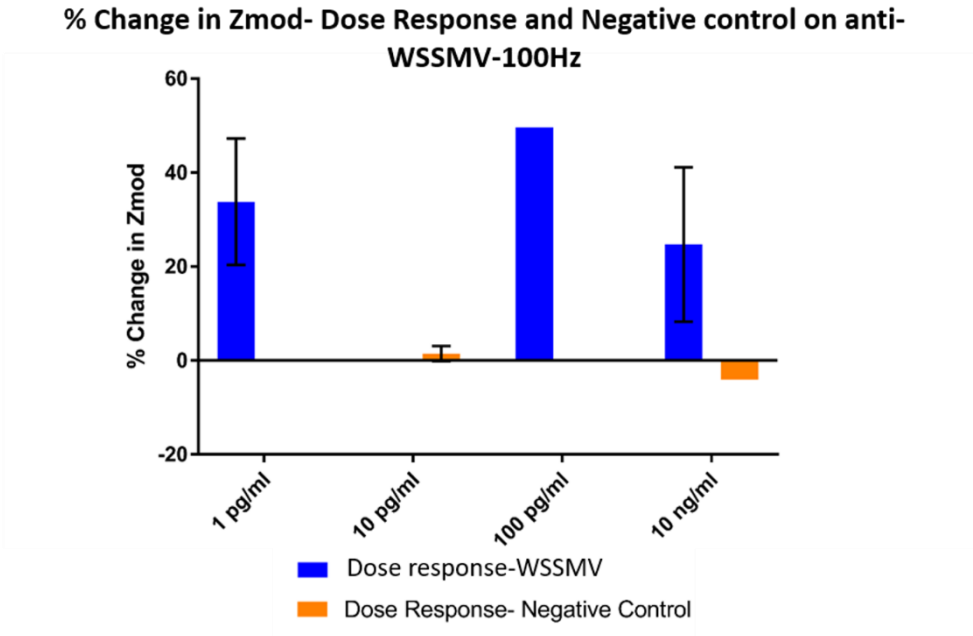

Figure 4.13: Raw dose response of wheat spindle streak mosaic virus (WSSMV) at 100 Hz

error bars were performed for n=2 replicates. For the positive control, the doses do not show dose dependent change, however, with the end objective being just detection of the presence or absence of a virus for a field based application, it is sufficient to show the presence of the virus. The data processing step is just a method to present the data for ease of understanding. For the experiments performed on the other two immunoassays the raw representation of the data in terms of positive and negative controls is used. The results for the other two immunoassays are presented in the form of raw data and unprocessed as in the case of figure 4.13.

The data from the figure 4.14 shows a similar trend to that seen for WSSMV in figure 4.13, where the dose responses for both SBWMV and HPV, show a positive trend and a dose dependent change for the dose response. The dose response in the case of HPV, depicted by part i. of figure 4.14, is seen to have a dose dependent change.

The maximum positive dose response seen is for the range of 10-100 ng/mL, which is the high concentration range. The negative control shows a completely opposite trend, also dose dependent change, with a maximum change of -28% for the high concentration range. In part ii. of the figure 4.14, a dose dependent change is seen for the dose response for SBWMV, with a maximum positive change of 9%.

Again, for the negative control, a negative trend is seen with a maximum change of -18% for the middle concentration range of 100pg/mL-1ng/mL.

Since the positive and negative controls show opposite trends due to the reasons discussed, we can lean towards the conclusion that binding occurs and therefore both SBWMV and HPV is detected on the addition of a discreet dose. For the data represented in the figure 4.12, we can

safely conclude that WSSMV is being detected after normalization of the data. However, applying the same method for the other two molecules of interest does not produce the exact

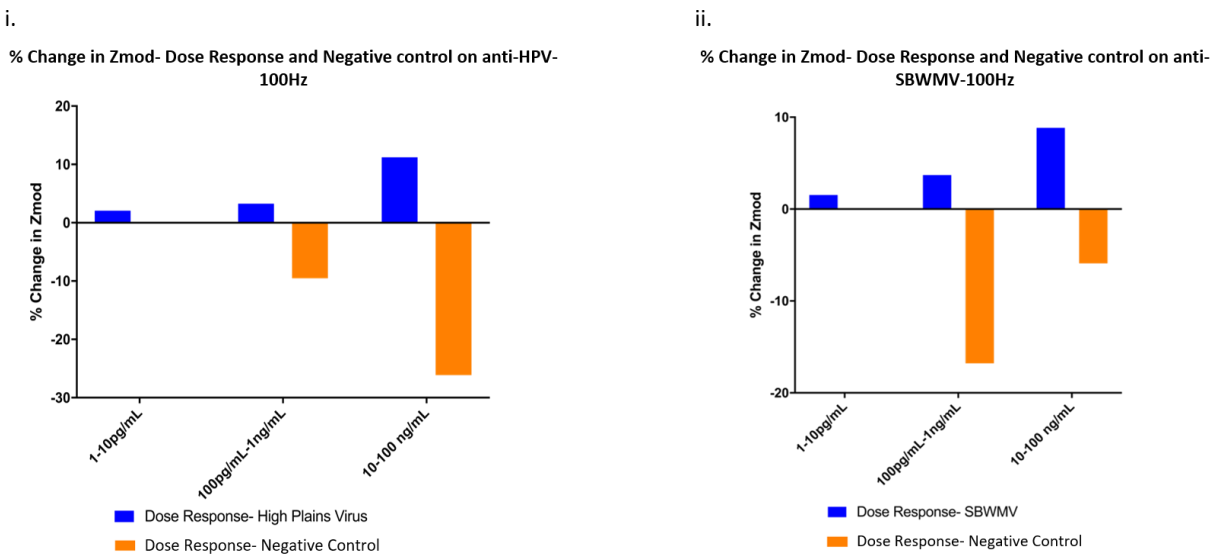

Figure 4.14: Raw dose response of HPV and SBWMV at 100Hz

results that is expected to be seen. Repeatability is the best way to get better and more desirable results and work is in progress for the same.

CHAPTER 5

CONCLUSIONS

Preliminary work for the ultrasensitive field based biosensor towards the multiplexed detection of wheat pathogens in a complex buffer is developed. Various aspects of electrode design are studied and an electrode of suitable size, surface area and volume is chosen for the detection of wheat pathogen in plant sap. This particular sensor has many advantages over the current existing technology, in today's market. Some of the advantages include: 1) it is label-free, hence no external tags are required, which also reduces risk of contamination of the immunoassay; 2) it has been devised to function as a portable device which was one of the primary objectives of this work; 3) it is a low cost manufacturing process; 4) rapid response time, with results in 30 minutes; 5) its low limit of detection and ultra sensitivity means that it is 100 times more sensitive than the available techniques; 6) it requires extremely low sample volumes to perform a complete test.

The binding of the linker, antibody and antigen is established making it a stable and robust biosensor. The establishment of dose dependent response, sensor parameters such as dynamic range, SNR, limit of detection (LoD) and limit of blank (Lob) for both simple and complex buffer is established.

Cost effective, portable, rapid multiplexed plant pathogen screening using small volumes of sample is essential and is a necessity in today's world and the biosensor developed fulfills the requirements for pursuing a true field based plant pathogen sensor-SapSense is here.

CHAPTER 6

FUTURE WORK

One of the first thoughts that come to mind on reading this thesis is that, the work focuses on a very specific plant-wheat and has a focus towards only three strains of viruses that affect wheat. The work presented in this thesis, establishes the proof of concept, by picking an instance of a plant pathogen that has a massive significance, which is already discussed in chapter 1 of this thesis. The ultimate aim is to be able to detect various other pathogens- bacteria, other plant viruses, using affinity based biosensors, which is definitely work for the future and the most economical technique moving forward. The sensor presented in this thesis is the first of its kind in the agriculture realm and will serve as the pathway to go for in the future for rapid, economical and accurate diagnosis.

The sensor upon integration into a drone like system, could be useful, to navigate and collect samples from various parts of the field and testing random samples. Another possible avenue to explore would be to design a multiplexed sensor as seen in design versions 1 and 2, presented in this work to detect multiple pathogen on the same sensor. There are multiple methods to implement the construction of the bio-sensor.

The sensor is currently tested on a standard benchtop potentiostat. Another potential improvement would see the sensor interfaced with a portable potentiostat which is capable of producing results in the field. Further instrumentation can be developed for this kind of sensor device, with the use of microcontrollers to make it an application specific device.

REFERENCES

[1] P. R. Shewry, “Wheat.,” *Journal of experimental botany*, vol. 60.6, pp. 1537-1553, 2009.

[2] J. D. Mauseth, Botany, Jones & Bartlett Publishers, 2014.

[3] B. Belderok, Bread-making quality of wheat: a century of breeding in Europe., Springer Science & Business Media,, 2000.

[4] M. Feldman, "Domestication of emmer wheat and evolution of free-threshing tetraploid wheat," *Israel Journal of Plant Sciences,* vol. 55.3, pp. 207-221, 2007.

[5] S. Colledge, The origins and spread of domestic plants in Southwest Asia and Europe, Left Coast Press,, 2007.

[6] Food and Agriculture Organization, "World food situation: FAO cereal supply and demand brief," United Nations, 8 December 2016. [Online]. Available: http://www.fao.org/worldfoodsituation/csdb/en/.

[7] R. Curtis, "" Bread Wheat”. Food and Agriculture Organization of the United Nations," *MacPherson,* 2002.

[8] Food and Agriculture Organization, "FAO Cereal Supply and Demand Brief," Food and Agriculture Organization of the United Nations, June 2017. [Online]. Available: http://www.fao.org/worldfoodsituation/csdb/en/. [Accessed 14 August 2017].

[9] A. Bekkerman, "Forecasting a moving target: The roles of quality and timing for determining northern US wheat basis," *Journal of agricultural and resource economics,* vol. 41.1, pp. 25-41, 2016.

[10] M. Burrows, "Coordination of Diagnostic Efforts in the Great Plains: Wheat Virus Survey and Modeling of Disease Onset.," *Plant Disease,* vol. 100.6, pp. 1037-1045, 2016.

[11] E. Oerke, "Crop losses to pests," *The Journal of Agricultural Science,* vol. 144.1, pp. 31-43, 2006.

[12] S. Savary, Crop losses due to diseases and their implications for global food production losses and food security, Springer, 2012, pp. 519-537.

[13] P. Christou, "The potential of genetically enhanced plants to address food insecurity," *Nutrition research reviews,* vol. 17.1, pp. 23-42, 2004.

[14] U. Nations, The state of food security in the world, Food and Agriculture Organization of the United Nations, 2000.

[15] Agricultural Marketting Resource Center, "Wheat- Agricultural marketting resoucre center," Agricultural marketting resoucre center, 2017. [Online]. Available: http://www.agmrc.org/commodities-products/grains-oilseeds/wheat/.

[16] R. W. Christina Cowger, "United states department of agriculture- agricultural research service," 2005. [Online]. Available: https://www.ars.usda.gov/ARSUserFiles/60701500/Publications/Cowger/CowgerWeisz05.pdf.

[17] J. Te, "Soilborne wheat mosaic virus (SBWMV) 19K protein belongs to a class of cysteine rich proteins that suppress RNA silencing.," *Virology journal,* vol. 2.1, 2005.

[18] A. Ziegler, "Occurrence of the New York Strain of Soil-Borne Wheat Mosaic Virus in Northern Germany," *Journal of Phytopathology,* vol. 161.4, pp. 290-292, 2013.

[19] R. L. Bowden, "Factsheet- Wheat- Wheat spindle streak mosaic virus," june 2000. [Online]. Available: http://www.plantpath.k-state.edu/extension/publications/wheat-spindle-streakmosaicvirus.pdf.

[20] B. A. R. Hadi, "Wheat streak mosaic virus on wheat: biology and management.," *Journal of Integrated Pest Management,* vol. 2.1, 2011.

[21] B. A. R. Hadi, "Wheat streak mosaic virus on wheat: biology and management," *Journal of Integrated Pest Management,* vol. 2.1, 2011.

[22] L. R. Stewart, "Wheat mosaic virus (WMoV), the causal agent of High Plains disease, is present in Ohio wheat fields.," *Plant Disease,* vol. 97.8, p. 1125, 2013.

[23] R. L. Bowden, "Factsheets-Wheat- Highplains Vrius on Wheat and Corn," June 2000. [Online]. Available: http://www.plantpath.k-state.edu/extension/publications/highplainsvirus.pdf.

[24] R. O'Kennedy, "Experimental section: a review of enzyme-immunoassay and a description of a competitive enzyme-linked immunosorbent assay for the detection of immunoglobulin concentrations," *Biochemical Education,* vol. 18.3, pp. 136-140, 1990.

[25] S. Aydin, "A short history, principles, and types of ELISA, and our laboratory experience with peptide/protein analyses using ELISA," *Peptides,* vol. 72, pp. 4-15, 2015.

[26] E. Engvall, "Enzyme-linked immunosorbent assay, ELISA," *The Journal of Immunology,* vol. 109.1, pp. 129-135, 1972.

[27] H. Y. Cai, "Nonculture molecular techniques for diagnosis of bacterial disease in animals: a diagnostic laboratory perspective," *Veterinary pathology,* vol. 51.2, pp. 341-350, 2014.

[28] J. M. Logan, Real-time PCR: current technology and applications., Horizon Scientific Press, 2009.

[29] H. Towbin, "Electrophoretic transfer of proteins from polyacrylamide gels to nitrocellulose sheets: procedure and some applications," *Proceedings of the National Academy of Sciences,* vol. 76.9, pp. 4350-4354, 1979.

[30] J. Renart, "Transfer of proteins from gels to diazobenzyloxymethyl-paper and detection with antisera: a method for studying antibody specificity and antigen structure.," *Proceedings of the National Academy of Sciences,* vol. 76.7, pp. 3116-3120, 1979.

[31] M. E. Orazem, An Integrated Approach to Impedance Spectroscopy: Electrochemical Impedance Spectroscopy, Wiley, 2008.

[32] J. R. Macdonald, Fundamentals of impedance spectroscopy Impedance Spectroscopy: Theory, Experiment, and Applications, Second Edition, John Wiley & Sons, 2005.

[33] E. Randviir, "Electrochemical impedance spectroscopy: an overview of bioanalytical applications," *Analytical Methods,* vol. 5.5, pp. 1098-1115, 2013.

[34] A. P. Selvam, "Design of a high sensitive non-faradaic impedimetric sensor.," *Engineering in Medicine and Biology Society (EMBC), 2012 Annual International Conference of the IEEE,* 2012.

[35] A. Santos, "Fundamentals and applications of impedimetric and redox capacitive biosensors.," *Journal of Analytical & Bioanalytical Techniques,* vol. 57, 2015.

[36] P. Daniels, "Label-free impedance biosensors: Opportunities and challenges.," *Electroanalysis,* vol. 19.12, pp. 1239-1257, 2007.

[37] D. R. Thévenot, "Electrochemical biosensors: recommended definitions and classification," *Biosensors and Bioelectronics,* vol. 16.1, pp. 121-131, 2001.

[38] T. G. Drummond, "Electrochemical DNA sensors," *Nature biotechnology,* vol. 21.10, p. 1192, 2003.

[39] T. D. Bakker, "Electrochemical sensors," *Analytical chemistry,* vol. 74.12, pp. 2781-2800., 2002.

[40] M. Jacobs, "Ultra-sensitive electrical immunoassay biosensors using nanotextured zinc oxide thin films on printed circuit board platforms.," *Biosensors and Bioelectronics,* vol. 55, pp. 7-13, 2014.

[41] V. J. Nagaraj, "Nanochannel-based electrochemical sensor for the detection of pharmaceutical contaminants in water.," *Environmental Science: Processes & Impacts,* vol. 16.1, pp. 135-140, 2014.

[42] S. K. Arya, "Antibody modified gold micro array electrode based electrochemical immunosensor for ultrasensitive detection of cortisol in saliva and ISF.," *Procedia Engineering 5,* pp. 804-807, 2010.

[43] F. A. Lomant, "Chemical probes of extended biological structures: synthesis and properties of the cleavable protein cross-linking reagent [35S] dithiobis (succinimidyl propionate).," *Journal of molecular biology,* pp. 243-261, 1976.

[44] H. Marschner, "General introduction to the mineral nutrition of plants," *Inorganic plant nutrition. Springer Berlin Heidelberg,* pp. 5-60, 1983.

[45] A. Khan, Plant anatomy and physiology, Gyan Publishing House, 2002.

[46] C. L. Morgan, "Immunosensors: technology and opportunities in laboratory medicine.," *Clinical chemistry,* vol. 42, no. 2, pp. 193-209, 1996.

[47] T. S. Pierce, "antibody production and purification technical handbook," [Online]. Available: https://tools.thermofisher.com/content/sfs/brochures/1601975-Antibody-Production-Purification-Guide.pdf.

[48] J. C. Jr, Immunobiology: The Immune System in Health and Disease, New York: Garland Science, 2001.

[49] V. J. Nagaraj, "Nanochannel-based electrochemical sensor for the detection of pharmaceutical contaminants in water," *Environmental Science: Processes & Impacts,* vol. 16.1, pp. 135-140, 2014.

[50] M. Jacobs, "An electrochemical sensor for the detection of antibiotic contaminants in water," *Analytical Methods,* vol. 5.17, pp. 4325-4329, 2013.

[51] D. A. Armbruster, "Limit of blank, limit of detection and limit of quantitation.," *The Clinical Biochemist Reviews,* vol. 29, no. 1, 2008.

[52] A. Shrivastava, "Methods for the determination of limit of detection and limit of quantitation of the analytical methods.," *Chronicles of Young Scientists,* vol. 2.1, 2011.

[53] J. S. E. A. Daniels, "Simultaneous measurement of nonlinearity and electrochemical impedance for protein sensing using two-tone excitation.," *Engineering in Medicine and Biology Society,* 2008.

[54] Macrotrends, "Wheat Prices-40 year historical chart," Macrotrends, 2017. [Online]. Available: http://www.macrotrends.net/2534/wheat-prices-historical-chart-data.

[55] T. Murray, "First Report of Soilborne wheat mosaic virus on Triticum aestivum in Washington State," December 2009. [Online]. Available: https://www.plantmanagementnetwork.org/elements/view.aspx?ID=4704.

[56] "Helping Wheat Defend Itself Against Damaging Viruses," November 2014. [Online]. Available: http://www.newswise.com/articles/helping-wheat-defend-itself-against-damaging-viruses.

[57] Wikipedia, "ELISA," September 2017. [Online]. Available: https://en.wikipedia.org/wiki/ELISA#/media/File:ELISA_diagram.png.

[58] T. Murray, "First Report of Soilborne wheat mosaic virus on Triticum aestivum in Washington State," December 2009. [Online]. Available: http://www.plantmanagementnetwork.org/pub/php/brief/2009/sbwmv/.

[59] Newswise, "Helping Wheat Defend Itself Against Damaging Viruses," November 2014. [Online]. Available: http://www.newswise.com/articles/helping-wheat-defend-itself-against-damaging-viruses.

[60] T. F. Scientific, "PCR Cycling Parameters—Six Key Considerations for Success," Thermo Fisher Scientific, September 2017. [Online]. Available: https://www.thermofisher.com/io/en/home/life-science/cloning/cloning-learning-center/invitrogen-school-of-molecular-biology/pcr-education/pcr-reagents-enzymes/pcr-cycling-considerations.html.

BIOGRAPHICAL SKETCH

Akshay Vasudevan received his Bachelor of Engineering in Biomedical Electronics from the Dayananda Sagar College of Engineering, India, in the summer of 2014, graduating with distinction. As an undergraduate, he was awarded a grant for his senior design project, from the Department of Science and Technology, Government of India, for his research in the field of rural rehabilitation. He joined the graduate program for bioengineering at The University of Texas at Dallas in fall 2015. During his time as a graduate student, he joined the Biomedical Microdevices and Nanotechnology Lab (BMNL) in the summer of 2016, under the guidance of Dr. Shalini Prasad and served as a teaching assistant for two semesters. Currently, he has been working on building a unique bio-sensing platform, which is a filed based bio-sensor, towards the detection of wheat pathogen.

CURRICULUM VITAE

AKSHAY VASUDEVAN

EDUCATION:

The University of Texas at Dallas, Richardson, Tx **Dec 2017**

Master of Science- Biomedical Engineering

Visveswaraya Technological University, Bangalore, India **May 2014**

Bachelor of Engineering- Medical Electronics Engineering

TECHNICAL SKILLS:

Languages Turbo C, C++, MATLAB, Assembly, Verilog, HDL, R/Rattle, Java

Software Arduino, MATLAB and Simulink, LabView, SolidWorks, AutoCad, Eagle, Xilinx, Comsol Multiphysics, Graphpad-prism, MS Office

WORK EXPERIENCE:

- **Graduate Teaching Assistant, University of Texas at Dallas** **Aug 2016 - Aug 2017**

Advanced MATLAB for Biomedical Engineering; Biomedical Components and Circuits Laboratory

- **Graduate Research Assistant, University of Texas at Dallas** **May 2016-Dec 2017**

Developed multiple projects, end-to-end, involving the design of experiments, data acquisition, data investigation, analysis and interpretation at Biomedical Microdevices and Nanotechnology Laboratory

- **VMware Solutions India Private Ltd, Bangalore** **Aug 2014-July 2015**

Solutions Engineer- Troubleshoot, supported and resolved core product issues for Vsphere, Vcenter Server and VMware ESX(i) server software 4.X/5.X

- **Intern-Junior Biomedical Technician, Sagar Hospitals, Bangalore Aug 2013- Dec 2013**

Diagnosed, troubleshoot, support and generate reports and records of CCU and emergency medical devices to improve the quality management of the systems

THESIS AND PUBLICATIONS: Dec 2017

"SapSense"- Development of a Field based Biosensor Towards Wheat Pathogen Detection
Engineered and evaluated sensor designs, using the principles of nanotechnology. Established the presence of plant pathogen by using Electrochemical impedance spectroscopy(EIS) and consequently diagnose the presence of disease within 30 minutes of screening, thereby helping reduce loses in yield and increase productivity

PROJECTS:

Evaluation of Diabetes Readmission and Cost Analysis-Healthcare Analytics

Feb 2017-May 2017

Predicted patient readmission and costs using 'Drug administered' as variables. Built Regression analysis decision tree, Random forest and Support Vector Machine models using R/Rattle. Results included predicting the drugs to incentivize using these models to reduce readmission and reduce cost to the insurance companies

Design of a flex-sensor for real time detection of neurotransmitters Jun 2016-Dec 2016

Designed flexible polyimide sensors detect the release of neurotransmitter (NT) in the brain using EIS and Cyclic Voltammetry. In-vitro results included the ability to distinguish different NTs including dopamine and acetylcholine

Modelling the Effects of Estrogen on the Wound Healing Processes Aug 2015-Jan 2016

Modelled the effect of estrogen and cortisol during the inflammatory phase of wound healing and predicted the speed of wound healing, per gender, age, and stress levels in the human body using MATLAB

AWARDS:

Department of Science and Technology (DST), Government of India Jul 2013-May 2014

Sá Sara- A Portable Assistant for Sitting and Standing: Received a cash award and led the senior design team to engineer a patient support system for the geriatric population as part of a rural rehabilitation project